RICE UNIVERSITY

Evaluating the Effects of Cell Sample Preparation on FTIR Cancer Detection

by

Sterling James Noelck

A THESIS SUBMITTED
IN PARTIAL FULFILLMENT OF THE
REQUIREMENTS FOR THE DEGREE

Master of Science

APPROVED, THESIS COMMITTEE

Dr. Rebekah Drezek, Chair
Professor of Bioengineering,
Professor of Electrical and Computer Engineering

Dr. Kevin Kelly
Associate Professor of Electrical and Computer Engineering

Dr. Junichiro Kono
Professor of Electrical and Computer Engineering

HOUSTON, TEXAS

April 2013

ABSTRACT

Evaluating the Effects of Cell Sample Preparation on FTIR Cancer Detection

by

Sterling James Noelck

This thesis examines some of the challenges involved with using FTIR spectroscopy for cancer detection including sample preparation and correcting for distortion from cell scattering. Sample preparation affects the spectra differently depending on the cell type, and can lead to significant changes in cancer biomarkers for a given cell type. Biomarkers derived from specific cancer types under one sample preparation are not reliable for other cancer types, and may not be suitable for the same cancer type using a different sample preparation. Cell scattering can also significantly affect the cell spectra, and as a result, correcting for the cell scattering distortion leads to changes in the biomarkers. For reliable cancer detection controlling variability is critical, especially in the complex spectra of biological samples. Standard sample preparation methods and scattering correction post-processing could improve comparison of cancer detection methods.

Acknowledgments

I would first like to my wife, Casey, who has been patient and understanding throughout my journey through graduate school at Rice, but especially in these last few months when I have been putting in extra hours to get everything done. She has provided much needed support for me when I had to make tough decisions. I would also like to thank my advisor Dr. Rebekah Drezek, who has been nothing but supportive of me throughout my time at Rice, even when things were not working, and also when I decided to switch majors. She has been more understanding than I could have hoped for in an advisor, and I want to thank her for time and commitment to helping me. I would like to thank Dr. Kevin Kelly for serving on my committee and for the discussions we had about school and what comes next. I would also like to thank Dr. Junichiro Kono for his willingness to serve on my committee and provide me with his insight. And finally I need to thank all the members of the Drezek lab who welcomed me into the lab and provided assistance and advice throughout my time here.

Table of Contents

List of Figures

Chapter 1

Current Cancer Detection Techniques

This thesis demonstrates the importance of correct sample preparation and the challenges faced when analyzing and comparing cell samples using Fourier transform infrared (FTIR) spectroscopy. Further, it goes on to demonstrate the varying effectiveness of FTIR spectroscopy to identify cancerous cells relying on multivariate peak analysis. The following section will document the both the importance of cancer detection, the benefits to FTIR spectroscopy as a tool to identify cancer, and the current progress in the field of FTIR cancer detection. This thesis focuses on using FTIR for identification of breast cancer and melanoma, so discussion will be mostly limited to those types of cancers.

1.1. Cancer Statistics

In 2012, in the United States an estimated 1.7 million people will be newly diagnosed with cancer, and cancer will kill approximately 600,000 people [1]. Cancer

accounted for roughly 1 out of every 4 deaths in 2010 and was the second leading cause of death behind heart disease; however, it has been closing the gap in recent years [2, 3]. Despite all of the advances in detection and treatment, cancer still remains difficult to diagnose and even more difficult to treat. However, early detection is very important and increases the chances for the patient to survive [1]. One of the benefits of FTIR spectroscopy is that it has the potential to identify cancers cells before changes are visible to pathologists using a standard Hemotoxin and Eosin H&E stain, currently the standard [4].

This project chose to focus on breast cancer and melanoma. Breast cancer was selected because it is the most common type of cancer in women, excluding basal and squamous skin cancer, and is a leading cause of cancer deaths in women, second only to lung cancer [1]. Melanoma was used because although it only makes up about 5-6% of skin cancer cases, it accounts for 75% of the deaths from skin cancer [5]. Skin cancer is very common, and despite being a small percentage of skin cancer cases, melanoma is the second most common invasive cancer in young adults behind breast cancer [6]. Another reason to look at melanoma is because of its location on the skin surface; this could offer a chance to test a future FTIR system as a non-invasive cancer screening tool

1.2. Breast Cancer

While early diagnosis of breast cancer is an important factor in decreasing the death rate from breast cancer, there is still much room for improvement [1, 7]. While FTIR has the potential to detect very early stage cancers because it collects information about the biochemical composition of the cells, early detection of breast cancer screening

is not the best application of FTIR spectroscopy because the cancer is too deep for non-invasive screening [8]. However, FTIR could be a potential tool in the assessment of breast cancer tumor margins, where it could be used to assess the removed tissue for cancerous regions.

1.2.1. Breast Cancer Tumor Margin Assessment

This section will describe the potential for FTIR spectroscopy to improve the outcome of tumor removal surgery by providing rapid analysis of excised tissue. After the removal of breast tissue the edges are inked, and the tissue is sent to be prepared to be sectioned and analyzed for the presence of cancer cells. Usually this process involves fixing the tissue in formalin and embedding it in paraffin for stability and long term storage and analysis. After these steps, an H&E stain is applied and a pathologist examines the tissue sections for the presence of cancer cells near the inked margin of tissue. If cancer cells are present at the inked edge, the tumor is considered to have 'positive' margins, which indicates that cancer cells likely remain in the patient. By this time the patient is 24-48 hours post-surgery, and depending on the situation may need to undergo an additional surgery or possibly just a more intensive radiation or chemotherapy regimen to remove or to try to kill the remaining cancer cells [9, 10]. Additional treatment is given to some patients with 'close' surgical margins; unfortunately, there is no clear definition of how to classify surgical margins. Commonly the margin is considered 'negative' or 'clear' if a certain distance exists between the tumor and the inked edge; if this gap is not present, but the cells do not reach the edge, the margin in considered 'close'. The distance required between the tumor and the edge for a classification of 'negative' can range from 1 mm to greater than 5 mm depending on the

institution [10]. Despite the debate of surgical margin status, it is considered to be the largest contributor to the risk of local recurrence, with positive margins increasing this risk [9, 10].

Tumor margins are mostly a concern in breast conservation therapy (BCT), where a small section of tissue including the tumor is removed. BCT has been in use since the 1960s for early stage breast cancer and has been shown to yield the same survival rate as a total mastectomy, which is the removal of the entire breast, including nipple and areola [11, 12]. For about two decades, BCT was the dominant choice for women undergoing surgery, but a study by McGuire et al. found that recently this trend had reversed and more women were opting for a total mastectomy. This preference for total mastectomy was stronger with young women (<40 years old) and women with a genetic mutation predisposing them to breast cancer. One of the main reasons for choosing a total mastectomy over BCT is the fear of recurrence, which is 2.3% and 8.8% respectively. The same study found that the patients opting for the total mastectomy reported having a higher quality of life following the surgery, presumably due to the reduction in their risk of a recurrence [13]. However, it is possible that a total mastectomy would not be necessary to assuage the fear of recurrence if the patients had the option of intraoperative margin assessment, which would determine the tumor status while the patient was still under anesthesia.

Currently intraoperative margin assessment is only available in specialized cancer centers, usually in the form of either touch prep cytology or frozen section histology, allowing them to get the results in less than 20 minutes [9]. These analyses allow the removal of additional tissue if needed to achieve negative tissue margins without the need

for a separate surgery [14]. In one study by Dener et al. of frozen sectioning, out of 190 tumors 30 patients had additional tissue removed to achieve negative margins. Of these 30, six patients required a mastectomy because of persistent positive or close margins while trying to do BCT. All the patients had a low rate of local recurrence (2.1%), which is similar to other studies of intraoperative margin analyses, which were also found to have lower rates of local recurrence when used to achieve negative margins rather than waiting for paraffin sectioning [14-16]. This rate of recurrence compares with the rate for a total mastectomy which would be reassuring to patients whose main reason for choosing a mastectomy is the fear of recurrence. This low rate of recurrence is one of the benefits of intraoperative analysis, which is so successful because it makes it possible to almost ensure the entire tumor is removed during the initial surgery. This removes the risks and physical and psychological stress of a second operation, usually following shortly after the recovery from the first, if the patient is even willing to undergo another operation so soon. Despite these advantages, intraoperative techniques are not widely employed because they require special equipment and trained pathologist to read the samples, which requires additional resources and adds to the cost of the procedure [15, 16]. One of the aims of this project is work toward a method of cancer detection that could be used intraoperatively without the need for extensive resources or expertise.

1.3. Melanoma

Melanoma would be a much better candidate for cancer screening using FTIR. There have been some FTIR studies that have shown differences between normal skin cells and melanoma, and Bhargava discusses the potential for FTIR screening of skin

cancers [17, 18]. While melanoma is not one of the more deadly cancers, a study found that the prevalence of melanoma in young adults has increased from a rate of 4.8 per 100,000 person-years age and sex corrected to the 2000 US white population between 1970-1979, to a rate of 30.8 between 2000-2009 [19]. This study was limited in scope and used regional data from Minnesota, but the trend is also seen at a national level, with an annual increase in incidences among Caucasians of greater than 60% in the past 30 years, and a rapid increase among young white women of 3 percent annually since 1992 [20]. While the incidence rates of melanoma are on the rise, the mortality rates have been decreasing, likely because of improved awareness and early detection [19, 21]. However, there is no clear consensus on the issue of routine screening for melanoma, with some organizations, American Academy of Dermatology and the American Cancer Society, recommending regular examinations, while the U.S. Preventive Services Task Force (USPTF) ruled in 2009 there was not enough evidence for a recommendation either way [5, 22]. Since most melanoma screenings are done by visual examination, they need to remove suspicious lesions for a biopsy to identify if it is cancerous or not. The USPTF's main claim is that there have not been enough quality studies on melanoma screening, benefits of early detection, and the potential drawbacks of screening to make a recommendation. If there were a non-invasive method of reliably testing suspicious lesions, it could greatly reduce the need for biopsies, thus reducing the cost and harm to the patient of screening.

Some studies have looked into new techniques for screening, including dermoscopy, the use of a low powered microscope to examine suspicious lesions without surface reflection, and visible/near infrared (NIR) spectroscopy of skin tissue, but neither

technique is widely used because of issues that will be discussed in the following section [23, 24]. One of the main problems with dermoscopy is that it is a subjective tool, and relies heavily on the experience of the person using it. Dermoscopy can improve diagnosis, but only when used by experienced experts. A study by Lorentzen et al. tested the effectiveness of dermoscopy by 'experts,' dermatologists who used it daily for 4-5 years, compared to 'non-experts,' residents with only 1-2 years' experience and formal training in dermoscopy. They found no difference in diagnostic ability over visual examination in the 'non-expert' group, but found a significant increase in sensitivity and specificity when used by the 'expert' group [25]. Melanin absorption spectroscopy is a method using visible/NIR spectroscopy to detect cancer by absorption profile, but it is still in early trials, so even if it proves to be reliable it will be some time before it becomes widespread [24]. FTIR spectroscopy could provide an objective diagnosis that does not rely on the users' expertise.

1.4. Current IR Cancer Detection Techniques

While FTIR spectroscopy is already in use for analysis of tissues and cells there is no standard method for sample preparation or post-processing. As FTIR spectroscopy becomes more common it is important that these issues are addressed. By collecting chemical information from the sample FTIR spectroscopy can identify cancer without the need for any labeling or contrast agents [4, 17, 18, 26]. In some cases, it can be used to detect differences in cancer cells even before morphological changes become visible using the standard H&E staining [4]. Yet, without any standardization it is difficult to compare all of the different methods and techniques used. FTIR spectroscopy of

biological samples usually ranges from the mid-IR region starting at 2.5 μm (4000 cm-1) out to around 10 μm (1000 cm-1), though some researchers sweep all the way out to 20 μm (500 cm-1). There are different ways to collect the FTIR spectra from samples and the method used can affect the shape of the resulting spectra [27, 28].

For biological samples spectra can be collecting using an attenuated total reflectance (ATR) attachment or probe, reflectance, transmittance, or even transflection (combination of reflectance and transmission). ATR uses a crystal with a high index of refraction that is pressed against the sample, light enters the crystal and is internally reflected creating an evanescent wave that interacts with the sample and allows the spectra to be collected. If the sample is a thick piece of tissue (> 5 μm), the best options are ATR or reflectance, because the signal would be too weak for transmission as light cannot penetrate the sample. ATR can also be done on thin samples because the penetration depth of the evanescent wave is generally between 0.5 μm and 2 μm, but reflectance does not work as well on thin samples because often too much light is transmitted and the reflected signal is weak. Transflectance can be used in this case, but one of the drawbacks to this method is that the signal is a combination of transmitted light and reflected light, which can make the signal harder to interpret [27, 28]. Transmission only works with thin samples because the signal has to pass through the sample to be detected. Some researchers employ FTIR spectroscopic imaging – sometimes called biospectroscopy or microspectroscopy – which is a technique of collecting the spectra from every pixel in the field of view. This technique has been explored for both digital histopathology – classifying cells and structures based on their spectra – and for identification of cancer cells among a mixed population [17, 29-32].

FTIR spectroscopic imaging is a powerful tool and shows promise in detecting breast micro-metastasis in the axillary lymph nodes, which are difficult to detect using standard histopathology due to the small size and lack of structure [33]. One of the limitations of FTIR spectroscopic imaging is that many instruments still rely on point scanning to create an image map, which can take up to 6 hours to obtain an image map of 100 spectra [32]. Despite the information rich images produced using this technique, point scanning is too time consuming for routine cancer detection. Improving MIR detector technology is reducing the cost of focal plane array (FPA) detectors while improving their noise characteristics, but the main advantage of using a FPA detector over single pixel detectors (SPD) is the time savings. For example, instead of collecting 256 spectra using point scanning in 4 hours, an FPA can collect 4096 spectra, at each pixel on the FPA, in just 5 minutes [30].

Researchers are using FPAs for IR imaging of large areas, greater than 30 μm x 30 μm, over point scanning with SPDs to allow for better spatial resolution and speed. While SPDs can offer a higher signal to noise (SNR) ratio than an FPA, they are less effective when scanning large areas because of errors caused by stage movement, non-equal throughput, and spatial resolution [34]. FPAs are still much more expensive than a comparable SPD, and the detector noise in some FPAs can be greater than all other sources of noise combined. Noise is an important consideration in the MIR because most IR sources are relatively dim, which makes getting a high SNR difficult, this becomes even more challenging when the light is split among the many pixels of an FPA detector [34]. One solution is to use a synchrotron, which is a particle accelerator that can be used as a bright source, to improve the SNR and even enable better resolution; for example,

Gazi et al. and Nasse et al. have produced some images with diffraction limited resolution that can resolve subcellular components [35, 36]. However, a particle accelerator requires a large area, as well as millions of dollars to build, maintain, and run, which makes them extremely rare and not cost effective for general diagnostic use. Therefore, using a synchrotron is not an option for most hospitals, and even with access it would be impractical to use it for routine analysis of tissue samples. Still, most of the research in FTIR can be done with a conventional ceramic source, and the coarser spatial resolution limit will still be able to identify cancerous regions, which are generally at least a few micrometers in size [17].

This thesis looks at using a conventional FTIR source and ATR attachment along with relatively simple post-processing for cancer detection to allow for widespread use of the techniques described. Van den Driesche et al. designed a cancer detection system using a pair of light emitting diode (LED) IR sources, an LED-photodiode MIR detector, and a set of filters to calculate the absorption ratio of the symmetric to asymmetric CH2 stretching peaks [18]. Their paper describes an affordable cancer detection system built from easily obtainable components. However, one drawback of their analysis is that by design it focuses on using a single peak for detection, and while there have been a number of papers that use univariate analysis, with the variation in signals from different samples, many univariate analyses are less effective when employed in a wide population test [17]. Their method may be effective for certain cancers, or in small scale tests, but to achieve the consistency and reliability needed for large scale implementation, spectra analysis needs to include multiple peaks and peak ratios to reduce the effects of patient to patient variability. However, with the improvement in laser technologies, especially in

the MIR region, their system could easily be adapted to use bright tunable MIR quantum cascade lasers (QCL), that could improve the SNR and offer the potential to analyze a region of the IR. This would allow for the use of multivariate data analysis using a brighter source than the conventional ceramic FTIR. Bogomolny et al. use a series of biomarkers that could likely be covered using two tunable MIR quantum cascade lasers (QCLs); this would also cover the CH_2 stretch ratio that Van den Driesche discusses. The work in this paper is done using a conventional FTIR, but it was done with the idea of moving toward tunable laser sources. This paper will discuss the peak ratios used by Bogomolny and Van den Driesche for cancer detection and test their effectiveness with breast cancer. If these ratios are reliable at distinguishing cancer from normal cells it would be possible to build a system using a couple of tunable QCLs that would enable faster sampling with better resolution because of the improved brightness of the source.

.

Chapter 2

Sample Preparation

This chapter will describe the methods used for growing and preparing the cells for spectra collection and the theory behind each technique, and then the following chapter will detail the results and effects that each sample preparation had on the signal. Some preliminary sample preparation methods were tested using the breast cancer cell line SKBR3 and the non-tumorigenic transformed breast tissue line MCF10A, although most of the work discussed will include the melanoma cell lines WM-266-4 and G361 as well. First this section will detail the cell culture techniques used for all cell lines, and then the discussion will transition to the transfer of the cultured cells to the slides for FTIR spectroscopy.

The cell lines used in this report are: a HER-2 positive breast cancer line (SKBR3), a non-tumorigenic transformed epithelial breast cell line (MCF10A), a melanin producing malignant melanoma cell line (G361), a proteoglycan antigen producing metastatic malignant melanoma cell line (WM366-4) and finally a normal primary

melanocyte cell line (HEMa-LP, Life Technologies) The cell lines and materials were supplied by ATCC unless otherwise noted. All cell lines were cultured in a humidified incubator (5% CO2, 37 °C) in a growth media supplemented with 1% penicillin-streptomycin. SKBR3 and G361 cells were grown McCoy's 5A medium with 10% Fetal Bovine Serum (FBS), and the MCF10A cells were cultured in mammary epithelial basal medium, with a BulletKit (Lonza). The HEMa-LP cell line was grown in Medium 254 with human melanocyte growth supplement-2, PMA-free, all supplied by Life Technologies, and the WM-266-4 cells were cultured in Eagle's minimum essential medium with 10% FBS. However, due to issues with cell contamination and then poor cell growth of the HEMA-LP cell line not enough usable data was collected from this cell line so it will not be included in the analysis. Before sample preparation the cells were trypsinized to free them from the flasks, then they cells were spun down at 125 g for 5 min (180 g for 7 min. for the HEMA-LP cell line), and the media and trypsin supernate was removed.

This thesis tested a number of different preparation methods that have been used in literature, as well as trying a couple that have not discussed yet. Among the techniques tested were a few involving drying a solution with cells onto a slide including: suspending the cell is 1% Dulbecco's phosphate buffered saline solution without magnesium and calcium (DPBS) and drying, either using N2 gas or just air drying, fixing the cells with Cytofix and drying on a slide, and fixing the cells in Cytofix before spinning down and rinsing with deionized (DI) water prior to depositing on a slide to dry. A new technique was borrowed from imaging tissues, where the cells werre deposited onto a slide in DPBS, and a second slide (cooled in a ethanol/dry ice bath) was placed on

top along with a cooled metal bar to provide an additional heat sink. This cryofreezing technique was used on tissue to freeze a single layer of cells onto the slide while the rest of the tissue was peeled away [37]. Another method tried was growing the cells directly onto low-e infrared reflective (MirrIR) slides (Kevley Technologies). This chapter will discuss each preparation method in detail including the details of the techniques used to prepare the samples for FTIR analysis. The results and analysis of the sample preparation will be discussed in chapter 3.

2.1. Unfixed Samples in DPBS

The technique of suspending cells in DPBS then drying was used by a number of different groups. Some groups would dry the samples with N2 gas [8, 26]. While other groups just air dried the samples and stored them in a dessicator [4, 35, 38]. One group even rinsed with PBS then DI water before drying, this was not attempted because of concern that the unfixed cells may be damaged by suspension in DI water [39]. Both drying with N2 gas as well as air drying were tested to see if the method of drying the sample would affect the FTIR spectra. For this method, after removing the cell media, the cells were rinsed with 10 mL PBS to remove any remaining media and a small sample (100 μL) was removed for cell counting while the remainder was spun down again. The supernate was removed and the cells were resuspended in PBS. The concentration of cells used for this method varied and it was found that depending on the cell type a concentration of between 1 x 106 to 1 x 107 cells per mL was sufficient for collecting a spectrum. A suitable signal could be collected with a lower density of SkBr3 cells than MCF10A cells. Once the solution was diluted to the final concentration of cells 10 μL of

cell solution was placed on the slide, then N2 gas was used to dry the spot or the slide was set aside to air dry. Under a microscope, the drying patterns between the N2 gas and air drying procedure appear different, an effect likely caused by the differing rate of evaporation. However, when examining the ATR FTIR spectra, there appeared to be no significant difference between the drying methods. The drying method was tested primarily with the SkBr3 and MCF10A cell lines, but both of the melanoma cell line samples were consistent with the results from the breast cell lines. The drying method samples were collected using the GoldenGate ATR. The remainder of the experiments in this paper use the air drying method because of the more uniform drying pattern; the N2 gas dried sections of the sample faster than others, which led to the non-uniform distribution of crystals and cells.

2.2. Cryofreezing Cells onto Slide

This method was adapted from a method of removing a layer of endothelial cells from a heart valve. The original technique sandwiched tissue between two glass coverslips, one of which was cooled in an isopentane dry ice solution. A cold aluminum rod, stored in the isopentane solution, was used to apply pressure as well as keep the coverslip cold. After 3-5 seconds the coverslip was peeled off with the endothelial cells frozen to them, and were then immersion in a fixative solution or lysis buffer for RNA extraction [37]. However, when the technique was applied to cells, the cells attached to the slide, and appeared intact, but the cell density on the slide was very low. The cells were free to move in the solution, and as the solution was sandwiched between two slides, the cells were spread across most of the slide rather than being contained in a

small spot. This technique appears to work well only when the cells are constrained, as in tissue, but is not suitable for fixing cells in solution. This method is not discussed in the analysis section due to the low density coupled with the difficulty of finding a cluster of cells for FTIR sample collection

2.3. Growing Cells on Slides

A few groups grew cell directly on an IR transparent medium for sample collection, and another group grew cells on the IR reflective MirrIR slides [18, 40, 41]. This was initially tried with standard cell culture chamber slides (ATCC), to test the procedure. The cell layer was not thick enough to prevent the ATR signal from interacting with the glass slides, but some signal from the cells was present. The cells were then grown on MirrIR slides using a slide well sticker (VWR) to create a shallow well to hold the media. The cells were seeded at approximately 5 $x10^3$ cells / cm^2, and grown for 2 days before rinsing them. The cell were rinsed with PBS and dried, or rinsed with PBS then fixed in Cytofix and dried. The cells grew okay on the MirrIR slides, but did not attach securely and some were washed away when the samples were rinsed, despite carefully adding and removing the solution. When collecting samples, a pretty strong absorption from glass was noticed that drowned out the signal from the cells. When looking into this, a thesis on the degradation of the IR reflective layer of the MirrIR slides under aqueous conditions was found [42]. Further studies of cells grown on MirrIR slides were discontinued, however, Gazi et al. did not mention any problems with the degradation of the IR reflective film when they grew cells on MirrIR slides. The paper focused on tissue and used a SR microscope in reflection mode for single cell

imaging, which if tightly focused would not have much interaction with the slide itself [40].

A study by Petibois looking at suitable IR substrates found that there were only a few that met their requirements for biotoxicity and cell adhesion, Si-Fl, Si-O, Si_3N_4, Ge, and carbon graphite. However, each of these has its own drawbacks, either being very thin and fragile, having a high energy loss or being opaque to light [43]. While a couple of groups have grown cells on CaF_2, Petibois et al found CaF_2 to be somewhat toxic to cells, a poor substrate for cell adhesion, and the cut off around 1100 cm^{-1} misses some biologically important peaks [18, 43]. ZnSe was also found to be somewhat toxic and a poor substrate for cell adhesion, as well as being fragile, making it a poor choice for ATR FTIR sample collection. Considering these factors and difficulties in finding a suitable IR substrate, simpler methods of sample preparation were explored.

2.4. Fixing Cells in Cytofix

There were not any papers that tested the effect of drying the cells in the fixing solution, the papers found would rinse the cells with either PBS or DI water as discussed in the next section. Simply drying the cells in PBS could cause changes to occur in the cell, fixing the cell should prevent the drying process from affecting the cell shape or characteristics. For this procedure the cells were rinsed with 10 mL of DPBS and spun down, then fixed in Cytofix—PBS with 4% w/v paraformaldehyde—to a concentration of approximately 6 $x10^6$ cells/mL, for 20 minutes, and then 10 µL were deposited on slides for drying and analysis. To determine if the changes from the PBS to fixed and rinsed in

DI water were from the cell fixation or from the DI rinse, or a combination of both, fixed cells without any rinse were used.

2.5. Fixing in Cytofix Followed by DI rinse

Most of the articles that fixed their cells also rinsed them with DI water before analysis [Gazi 2004, Mazur 2012, Martin 2010]. One of the few papers looking at fixation found a DI rinse seemed to be a simple option that preserved the cells and did not have much effect on the spectra [35]. However, another found that while there were some small differences between fixed and unfixed samples the differences were slight compared to changes from disease [39]. As in the previous methods, the cells were rinsed in PBS to remove any remaining media. The cells were then fixed in 0.5 mL of Cytofix for 20 min. before being spun down at 125 xg for 2 min. to remove the excess fixative. The samples were then rinsed in 10 mL of DI water and a 100 μL sample was taken and diluted with 900 μL PBS for cell counting while the samples were spun down at 125 xg for 5 minutes. The supernate was removed and the cells were suspended in DI water to a concentration of around 6 x 10^6 cells/mL. Finally 10 μL were deposited on slides for drying and analysis.

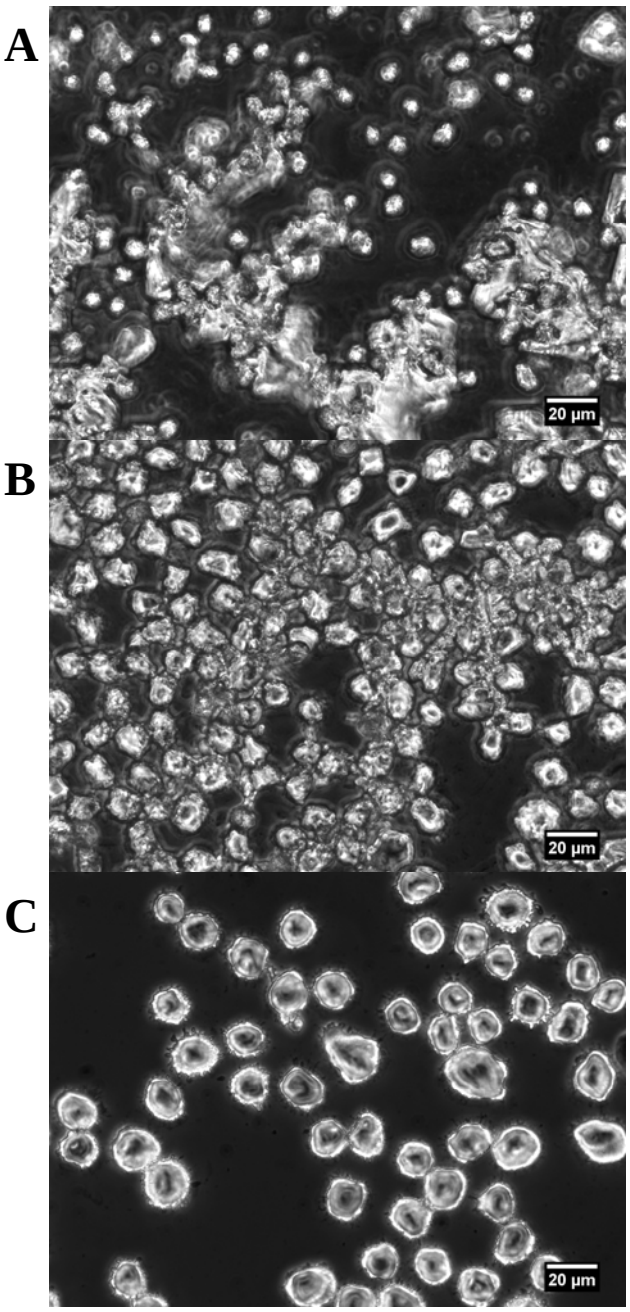

Figure 1. Bright field images of cell preparation, all samples were rinsed with PBS to remove any remaining cell media A) resuspended and dried in PBS, B) fixed and dried in Cytofix, C) fixed in Cytofix, rinsed with DI water, resuspended and dried in DI water

2.6. Other Sample Preparation Techniques

This section will describe some of the other techniques that have been used for FTIR imaging that were not repeated in this work. Gazi et al performed a study back in 2004 of fixation protocols using a synchrotron-based FTIR microscope, and they tested four different methods of fixation, formalin fixed cells rinsed in DI water and dried, washed in PBS and dried, and two different forms of critical point drying (CPD). One of the CPD techniques used cells fixed in formalin with the aqueous component replaced through 5-min immersions in increasing concentrations of ethanol (50%, 70%, 90%, and 100%). A 10-min immersion in cold acetone replaced the ethanol before the cells were loaded into the CPD chamber. Liquid CO_2 was then introduced for 15 minutes, then flushed out, repeated 2 more times to completely replace the acetone. By heating the cell to 45˚ C at a pressure of 108 bar, the air liquid interface disappears because of the phase transition of CO_2. The other CPD technique used a different fixation method using glutaraldehyde with a post-fixation treatment of osmium tetroxide before undergoing the same CPD treatment described above. They determined that the simpler and faster formalin-fixed method could enable high resolution spectroscopic images comparable or better than the CPD methods or the PBS drying [35]

Chapter 3

Effect of Sample Preparation on FTIR Spectra

This section will detail the procedure for sample collection and discuss the results and effects that the sample preparation had on the resulting spectra. This section will also discuss the differences seen across cell lines using the DI water rinse preparation and the difficulty in comparing FTIR spectra in the literature because of confounding factors.

3.1. Sample Collection Procedure

The samples were collected using a Nicolet Nexus 670 FTIR with a liquid N_2 cooled MCT/A detector and KBr beam splitter. The data was collected on two different ATR accessories, the first being a GoldenGate Smart ATR attachment with a diamond crystal, the second was a Smart iTR (Thermo-Fischer Scientific) with a diamond crystal. Both attachments are ATR modules and have similar characteristics, the main reason for the change was due to difficulty in collecting consistent spectra with the GoldenGate ATR. Two of the potential causes for the variability in sample collection using this

attachment are the inconsistency of the slip clutch at controlling the pressure applied to the sample, and the instability of the attachment itself in the FTIR machine, which could lead to laser misalignment. The first issue with the slip clutch was that it was sometimes difficult to know when it first engaged, and then after it engaged it was sometimes possible to increase the pressure slightly before the clutch would slip again. The GoldenGate ATR is old and the connections were worn, and did not fit tightly into the slots anymore, so the ATR could shift while changing samples. To minimize the effect of these issues the GoldenGate Smart ATR was stabilized before sampling began to reduce any movement and misalignment during sample collection, and the pressure was set as soon as the clutch slipped noticeably. The newer Smart iTR attachment fit securely into the FTIR without any movement or wobble, and the slip clutch reliably engaged with audible clicks and no additional pressure could be applied. The cell spectra collected with these attachments appeared to have a different shape; this could be due to differences in ATR design and/or differences in the experimental settings of each attachment. This project did not have the time to look into this result in detail, but this could be an area for further exploration.

With each attachment a background spectrum was collected with the crystal exposed to atmosphere before collecting cell spectra as described in [32] to account for any atmospheric absorption. Before each spectrum was collected, the background was checked to be flat before proceeding. Some artifacts appeared in the region of 2000 – 2500 cm^{-1} that were possibly due to atmospheric changes because they would appear as both peaks or dips throughout the sampling. These peaks were generally pretty small and could be ignored because there were no biologically important peaks in this region. If

peaks appeared in the background that remained after an additional cleaning of the crystal, a new background was taken before proceeding with sample collection. Initially the ATR crystal was cleaned with ethanol between each sample, but during the course of sample collection C-H stretching peaks would appear between 2850 and 2950, and a broader O-H stretch around 3300 that would slowly shrink again over the course of the next few samples – or would become dips over time if a new background was taken. These peaks are consistent with the chemical spectra of ethanol. One theory is that the ethanol could be trapped along the edges of the crystal – between the crystal and the plate – and would contribute slightly to the FTIR signal that would evaporate slowly. The procedure was changed to wiping off the crystal with a dry wipe between each sample, and confirming a flat baseline in the preview before collecting the next sample to ensure no sample to sample contamination. The crystal was cleaned with ethanol before and after each sampling run and allowed time to completely dry.

3.2. Sample Preparation Results

On visual inspection of the different sample preparations the formation of salt crystals in both the PBS and dried Cytofix – hereafter referred to as fixed – samples are obvious. These salt crystal can be seen in figure 1 (A) and (B), and the absence of them can be noted in (C). The crystals seen in these images are representative of around

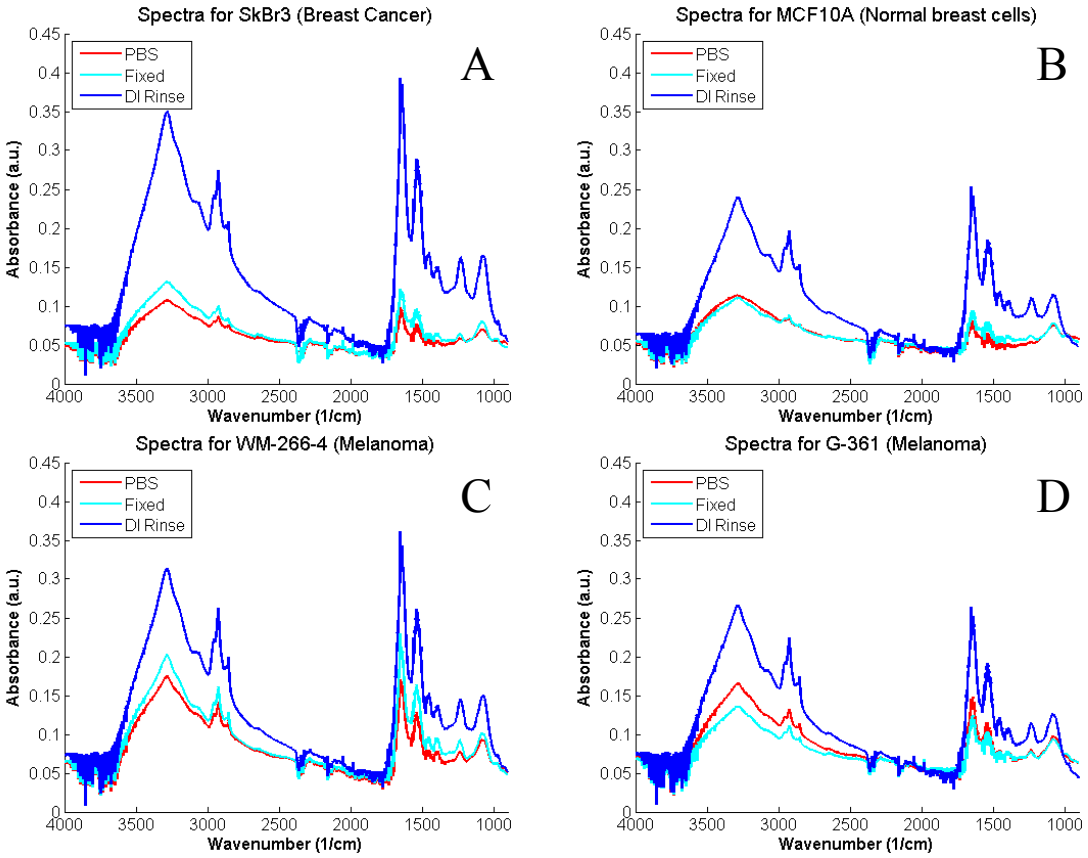

Figure 2. Spectra collected from different cell lines showing comparison of sample preparation. The largest signal was seen with the DI rinsed samples, more importantly peaks in the fingeprint region 1500-1000 are almost lost in some of the PBS and fixed samples. Spectra show the average signal from 15 samples for each preparation.

the average crystal size in the samples. However, some areas, generally toward the middle of the sample, contain much larger crystals which made it difficult to image the cells, this effect appears to be larger in the PBS samples than in the Cytofix samples. The crystals around the edge of the sample are usually smaller and less dense. This pattern reflects the air drying process with the water evaporating off initially from the edges and concentrating the salt content toward the middle of the sample. With the N_2 dried samples the crystals were less uniformly distributed due to uneven drying of the sample.

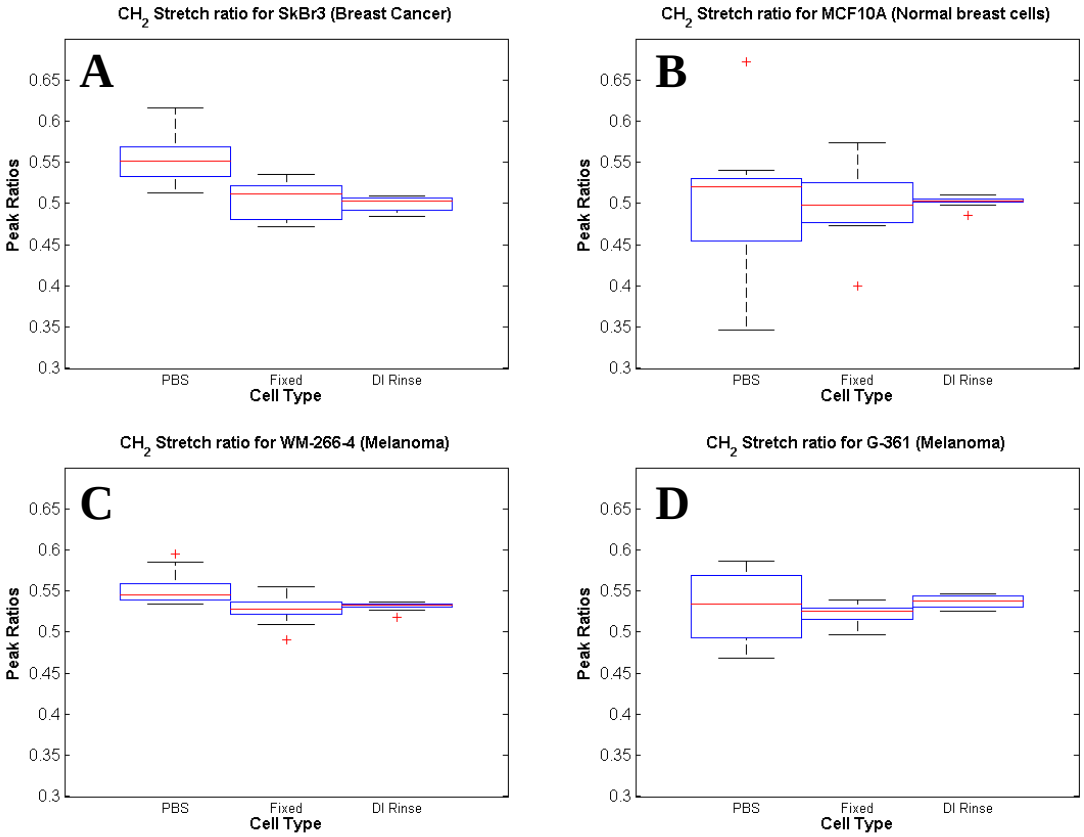

Figure 3. The effect of sample preparation on the symmetric to anti-symmetric CH_2 stretch ratio is not consistent across cell lines. In both the WM-266-4 and the SkBr3 cell lines, the PBS sample is significantly different than both the fixed and DI rinsed samples ($p < 0.05$), while there were no differences in either of the other two cell lines.

There is a clear difference in the magnitude of the FTIR signal of the DI water rinsed samples – later referred to as DI rinse – over both the PBS samples and the fixed samples (figure 2). Both the PBS and fixed spectra look similar so the salt crystals formed during the drying process may be contributing to the decreased signal. It is possible that the crystals could reduce the contact of the ATR crystal with the cells, or they may just scatter the IR light before it can interact with the cells. The reason was not able to be determined from these experiments. However, the magnitude is not the only

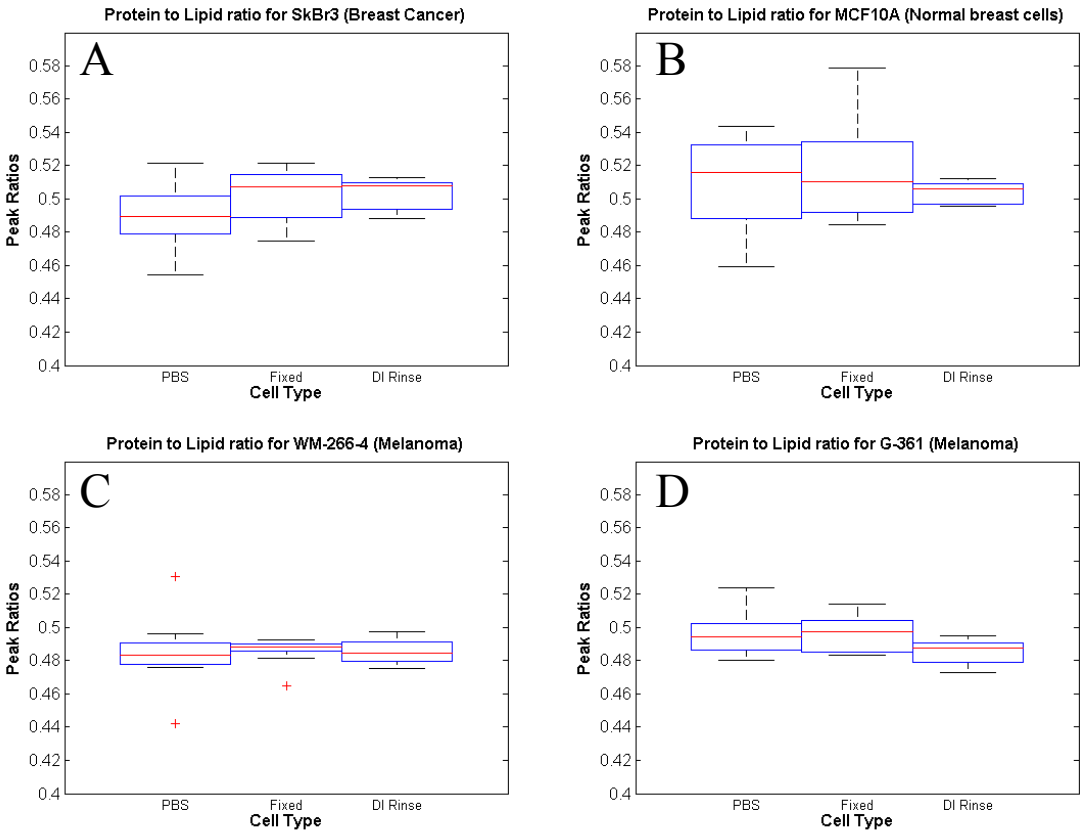

Figure 4. The sample preparation had no effect on the protein to lipid stretch ratio.

difference between the sample preparations, the peaks, especially in the 1000 cm^{-1} to 1500 cm^{-1} range are visually much larger and easier to distinguish in the DI sample. This can be seen much easier in figure 18 in Appendix A, which is zoomed in on this region. It appears that the sample preparation effect is larger in the breast cell lines than in the melanoma cell lines.

As this thesis explores FTIR spectroscopy as a potential tool for cancer detection, a set of peak ratios, or biomarkers, that have been used in literature to separate cancerous cells and tissue from normal were tested. The first biomarker, looking at the

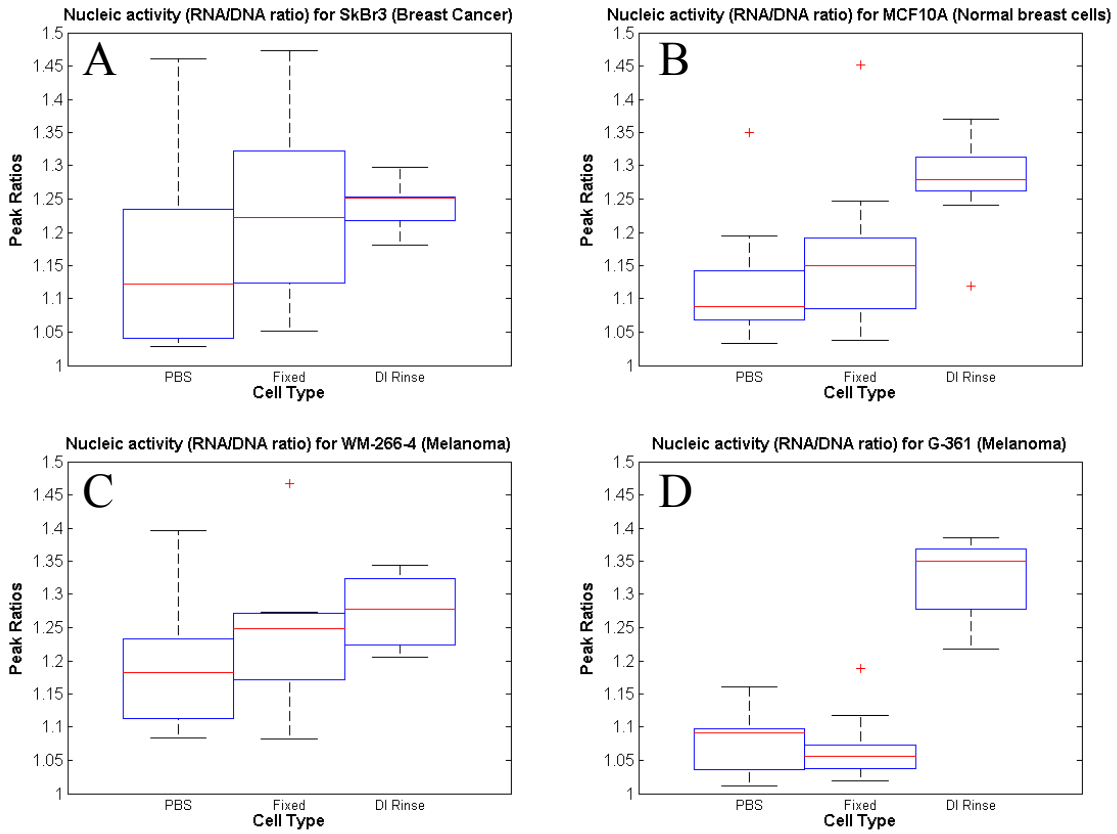

Figure 5. Sample preparation only effected the MCF10A and G-361 cell lines for the nucleic activity biomarker. The DI rinsed sample was significantly different than the PBS and fixed samples ($p < 0.05$).

ratio of the CH2–symmetric stretch to the CH_2–antisymmetric stretch, from van den Driesche et al., used four wavelengths between 3.3 µm and 3.6 µm (in wavenumbers: 2999 cm^{-1}, 2928 cm^{-1}, 2853 cm^{-1}, and 2805 cm^{-1}). They used two points (2999 cm^{-1} and 2805 cm^{-1}) to create a baseline, and then calculated the peak heights above the baseline using the other two. This ratio was derived to differentiate epithelial kidney carcinoma and melanoma cell lines compared to normal epithelial kidney and primary melanocyte cell lines. They found that the cancer line had a higher ratio and attributed this to the formation of cholesterol rafts in the lipid membrane which results in an overall decrease

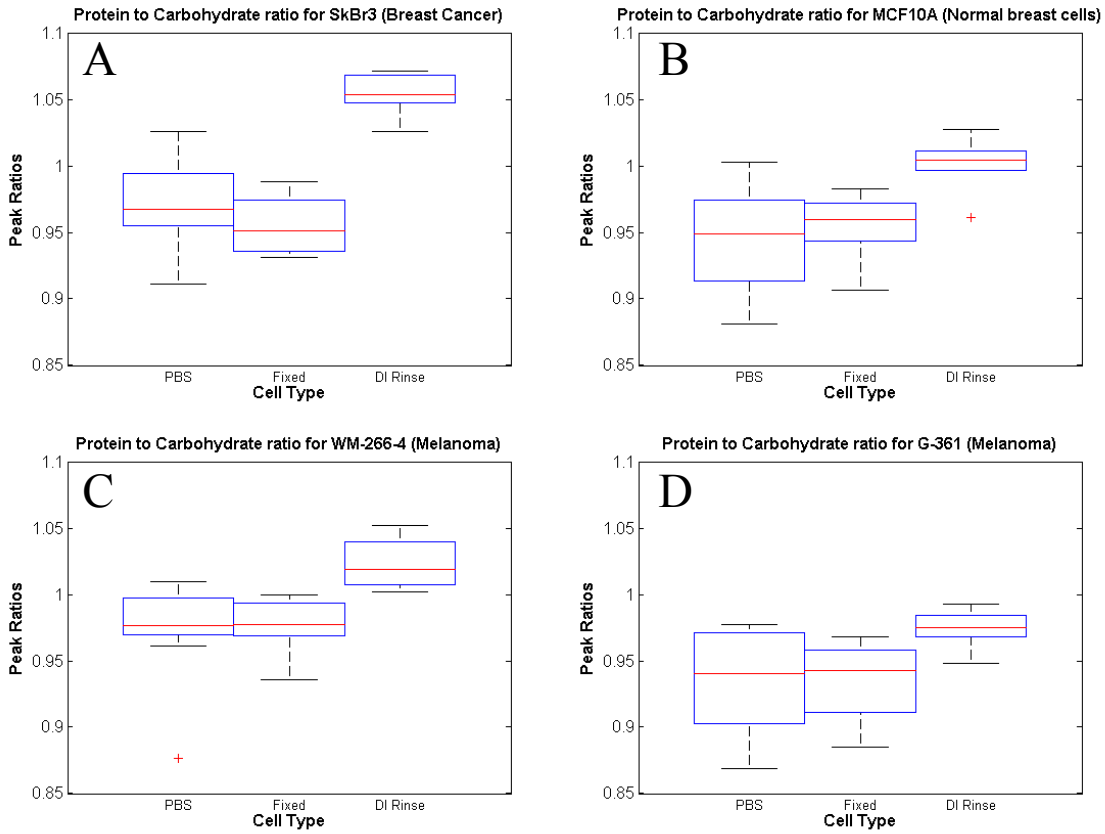

Figure 6. The DI rinse clearly had a strong effect on the protein to carbohydrate ratio. The DI rinsed sample ratios were significantly higher than the PBS and fixed ratios for all cell lines ($p < 0.05$).

in phospholipid organization [18]. The other biomarkers used were from Bogomolny et al. and their work on monitoring cancer progression in cervix tissue and transformed murine fibroblast and mouse embryonic fibroblast cell lines [4]. They used a set of four biomarkers to estimate the ratios of various cellular components, but did not use additional points to estimate a baseline, using instead a baseline corrected spectra using the rubber band method with 64 consecutive points. They looked at the protein to lipid ratio – 2958 cm^{-1}/ (2852 cm^{-1} + 2923 cm^{-1}) – the amount of nucleic activity, roughly the RNA/DNA ratio – 1121 cm^{-1}/1020 cm^{-1} – the protein to carbohydrate ratio –

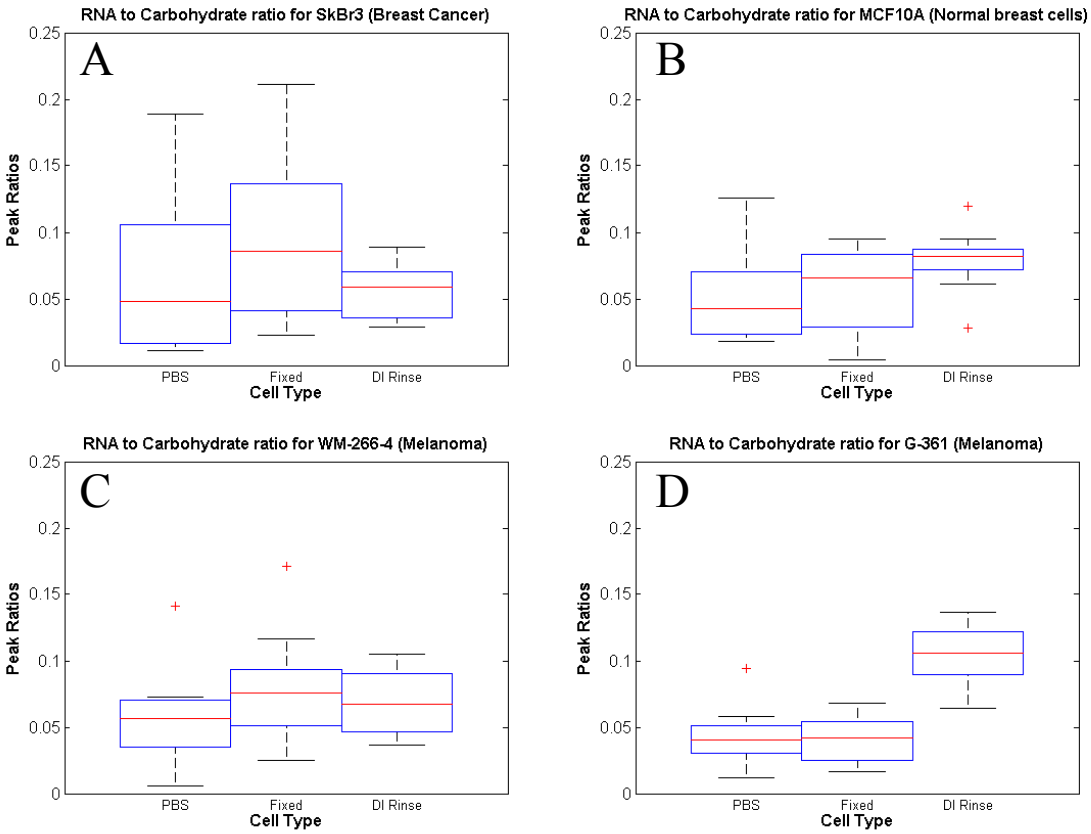

Figure 7. Only one cell line (G-361) showed significant changes from the sample preparation for the RNA to carbohydrate ratio biomarker ($p < 0.001$).

1171 cm^{-1}/ 1152 cm^{-1} – and the RNA to carbohydrate ratio – |1082 cm^{-1} - 1056 cm^{-1}| / 1028 cm^{-1} [4].

Altering the sample preparation can produce significant shifts in some of the biomarkers. More importantly the changes in the ratios of the biomarkers were not consistent across cell lines. The PBS sample ratio was significantly larger ($p < 0.005$) than both the fixed and DI rinsed samples for the CH_2 stretch ratio, in both the SkBr3 and WM-266-4 cell lines, while for the MCF10A and G-361 cell lines there was no change in this ratio (figure 3). There was no effect on protein to lipid ratio for any cell line (figure

4). In the nucleic activity biomarker (figure 5) the DI rinsed sample had the largest ratio, although the difference was only significant in the MCF10A and the G-361 samples ($p < 0.05$). For the protein to carbohydrate ratio (figure 6) the DI rinsed sample ratio was significantly higher across all cell lines ($p < 0.05$). Finally, in the RNA to carbohydrate ratio the DI rinsed sample ratio is significantly higher ($p < 0.001$) for the G-361 cell line, while there is no change among the other samples (figure 7).

The conclusion to take from this result is that sample preparation can have a significant effect on the FTIR spectra of biological samples, and the effect is not consistent across cell lines. It is important to understand that sample preparation could contribute to the FTIR signal when comparing results to other experiments. Some of the differences seen could be contributions from the sample preparations rather than solely due differences in the biological sample tested. It was decided that the DI rinse was the best method for further investigation. This decision was based on the absence of salt crystals, the larger and clearer signal of the DI rinsed samples – especially in the fingerprint region – and from the previous study [35, 39].

3.3. Comparison of Cell Lines using DI Rinsed Samples

Now that a sample preparation had been decided on, the next step was to compare the biomarkers with these cancer types and see if they could distinguish between the cell types. All of the spectra for the cell lines were collected with the Smart iTR FTIR

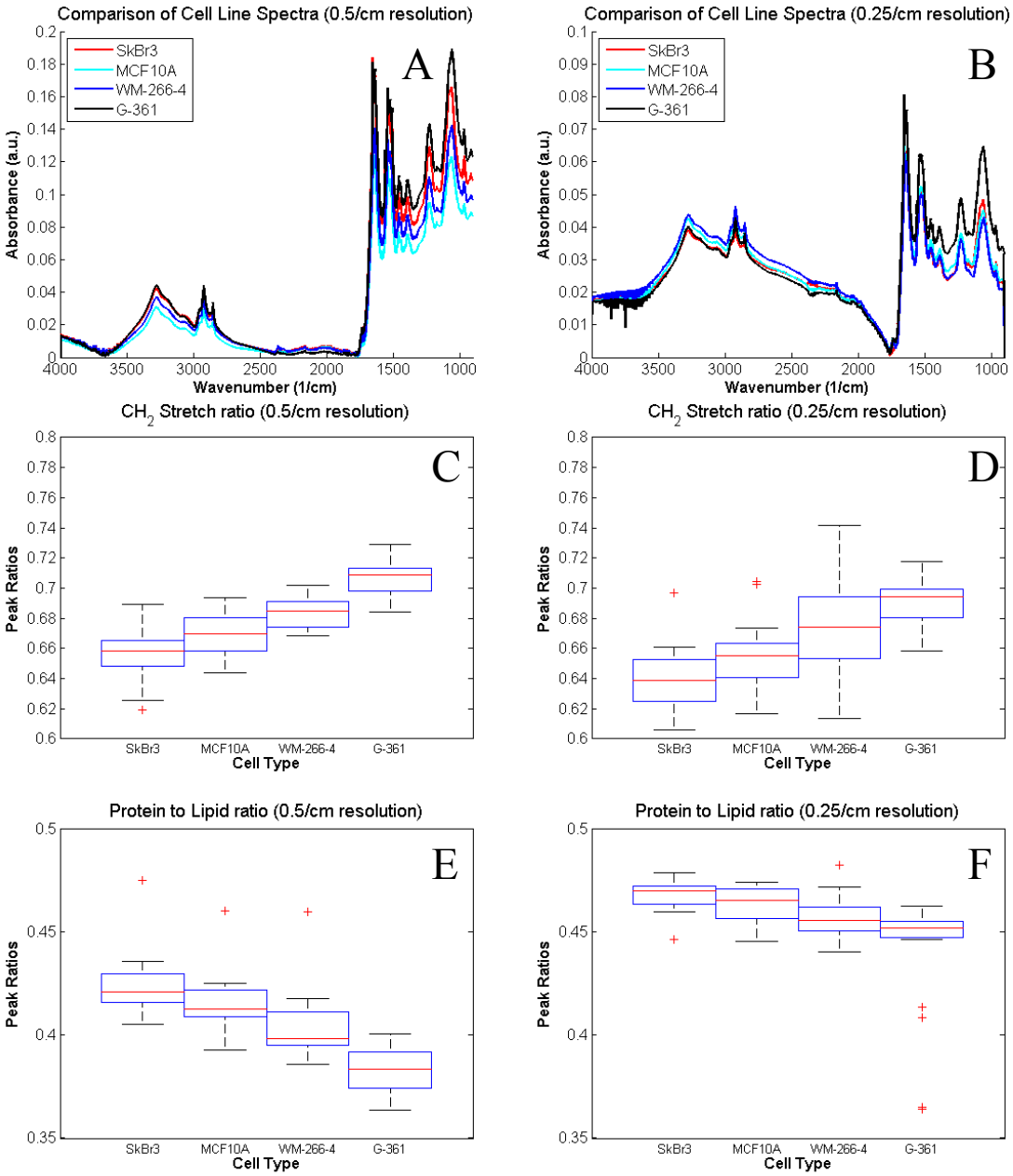

Figure 8. ATR spectra from all 4 cell lines using the DI rinsed samples at 0.5 cm^{-1} (A) and at 0.25 cm^{-1} (B). Comparison of CH_2 stretch ratio at 0.5 cm^{-1} (C) all cell lines were significantly different ($p < 0.05$) and for 0.25 cm^{-1} (D) both of the breast cell lines were lower than both melanoma cell lines ($p < 0.05$). In the protein to lipid ratio at 0.5 cm^{-1} (E) the G-361 cell line is significantly lower than all other cell lines ($p < 0.01$) and the WM-266-4 cell line is lower than the SkBr3 cell line ($p < 0.001$) and at 0.25 cm^{-1} (F) the G-361 cell line was lower than the other cell lines ($p < 0.05$).

attachment. The spectra were collected using 64 scans, with either a resolution of 0.5 cm^{-1} (sample spacing of 0.248 cm^{-1}) or .25 cm^{-1} resolution (spacing of 0.124 cm^{-1}) from 900 to 4000 cm^{-1}. Visually the spectra from the different cell lines look very similar, the peaks appear to be at the same locations, however the magnitude of the peaks differ between samples (Figure 8 A and B). The two sample collection runs were compared individually – each composed of 20 samples per cell type – and then combined the two to see how consistent the biomarkers were.

The first thing noticed was that the shapes of the spectra between the two runs were different, and this may have something to do with the lower signal strength in the higher resolution run or it may be from something else. These observations will be discussed in more detail in the next section. In terms of distinguishing the breast cancer from the normal breast cell line, the biomarkers were not very consistent, with the higher resolution run only finding the RNA to carbohydrate ratio (figure 9 F) to be significantly different ($p < 0.01$), while the lower resolution run found differences in the CH_2 stretch ($p < 0.05$), RNA to DNA ($p < 0.001$), and the RNA to carbohydrate ($p < 0.001$) ratios (figures 8C, 9A, and 9E).. The found the melanoma cell lines appeared to show the most promise for the use of these biomarkers. In the high resolution run the G-361 cell line was significantly different ($p < 0.05$), from the WM-266-4 cell line in all but the CH_2 stretch biomarker, and in the lower resolution run only the protein to carbohydrate and the RNA to carbohydrate ratios were not significant. In both runs the melanoma cell lines were usually different from both of the breast cell lines.

Comparing the two runs to each other, they show the same trends, with the main differences were that the lower resolution run generally had a couple more biomarkers

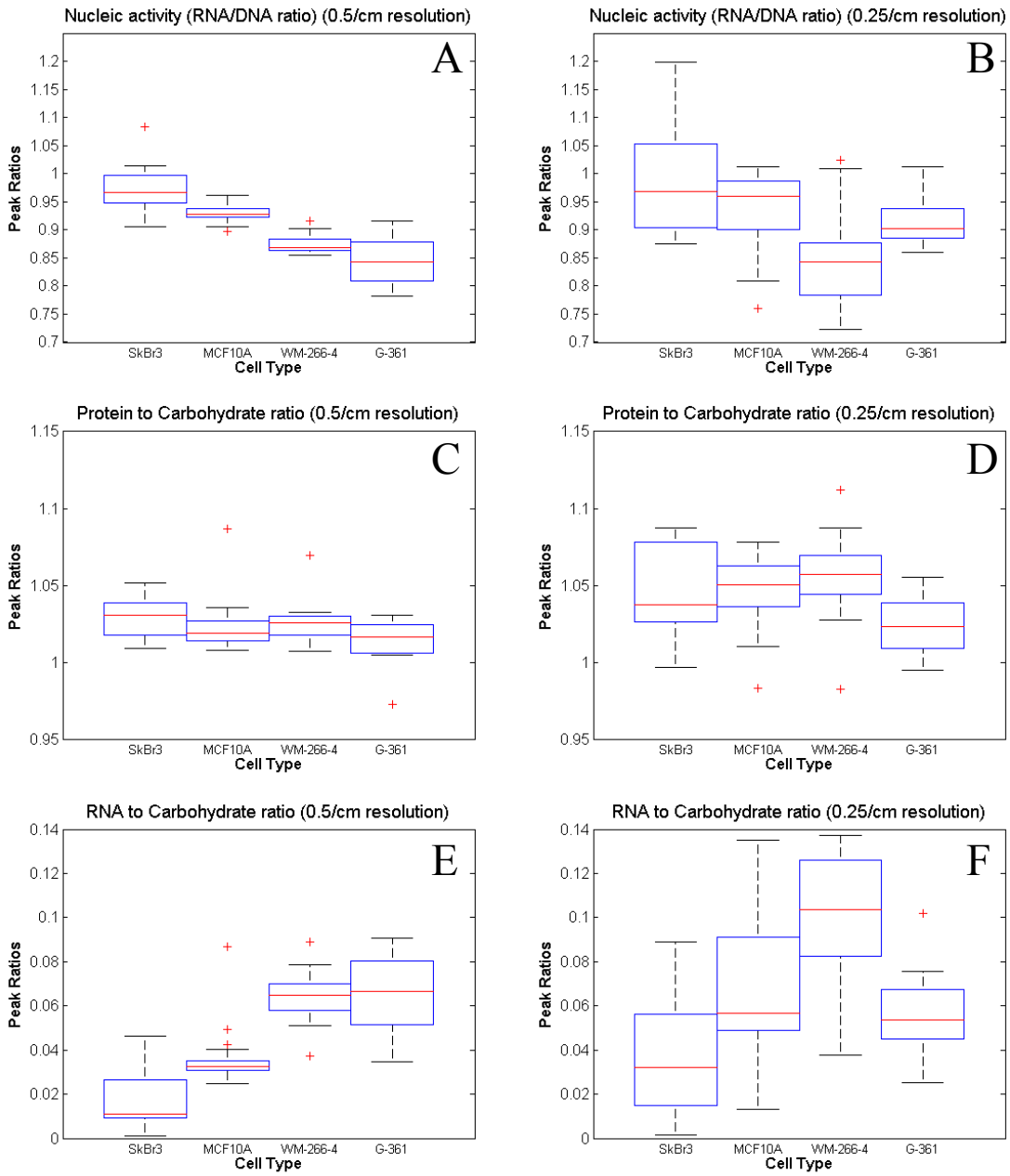

Figure 9. Biomarkers for DI rinse Nucleic activity for 0.5 cm^{-1} (A) all cell lines are significantly different ($p < 0.05$) and for 0.25 cm^{-1} (B) WM-266-4 is smaller than all other samples ($p < 0.05$) and G-361 is smaller than SkBr3 ($p < 0.05$). In the protein to carbohydrate ratio for 0.5 cm^{-1} (C) only the SkBr3 and G-361 cell lines are different ($p < 0.01$) and for 0.25 cm^{-1} (D) the G-361 cell line has a smaller ratio than all the other cell lines ($p < 0.05$). For the RNA to carbohydrate ratio with 0.5 cm^{-1} (E) both breast cell lines are lower than both melanoma lines, and the SkBr3 is lower than the MCF10A cell line ($p < 0.001$) and in the 0.25 cm^{-1} (F) WM-266-4 is the largest of all samples ($p < 0.001$), and SkBr3 was lower than MCF10A ($p < 0.01$).

that were significantly different, however in a couple of cases the higher resolution run had some biomarkers that were significant that were not seen in the lower resolution run. However, when the resolution was adjusted – by removing every other point so the sampling wavenumbers lined up – and the two runs were analyzed together, the results are very similar to the individual runs. There was one biomarker that was significant in both runs that was no longer significant when they were combined, but only two other biomarkers that were significant in either of the runs were not significant in the combined data.

Ultimately these results suggest that while these biomarkers may show significant differences between cell lines it would be difficult to rely only on these biomarkers for determining cancerous status. These biomarkers may have been selected to work with certain cancer types and do not work as well for other cancer types. It is also possible that by using a transformed cell line as a normal baseline, there could be some cancerous characteristics that are found in the FTIR spectra that do not manifest visually. FTIR analysis has been successfully used to distinguish cancer specimens in laboratory settings but there are still a number of issues to address before a simple FTIR cancer test can be used in a clinical setting.

3.4. Comparison of FTIR Settings and Attachments

During work with the GoldenGate ATR, issues were discovered with the stability and the slip clutch inconsistency which prompted the purchase of the Smart iTR, which is similar in design and application to the GoldenGate ATR. Despite their similarities, when samples were compared taken on the two different ATR attachments a trend was seen in

the spectra from the GoldenGate ATR compared to the spectra from the new Smart iTR. The GoldenGate ATR had much a much larger peak around 3300 cm^{-1} relative to the rest of the spectra. The cause of this is unknown and unfortunately there was not time to explore this further. A similar, though smaller, increase in the peak at 3300 cm^{-1} occurred in the higher resolution run Smart iTR. However this is likely due to some other reason because the samples on the GoldenGate ATR were collected at an even lower resolution (.482 cm^{-1}) than the samples collected on the Smart iTR (.248 cm^{-1} and .124 cm^{-1}). Not enough data was collected to know if the reason for the change was related to the resolution or not, but the samples were prepared identically but had much different spectral profiles. It would be interesting to see if changing the resolution consistently results in more than just a magnitude change in the spectra. If the resolution changes can change the spectral profile, it could have important implications for spectra analysis. It also means that reporting of resolution in FTIR papers would be even more important because if it had an effect on the shape of the spectra as well.

Chapter 4

Correcting for Cell Scattering

All of the above analysis was repeated again after using a resonant Mie scattering-extended multiplicative signal correction (RMieS-EMSC) algorithm developed by Bassan et al, to correct for cell scattering [44]. The algorithm is an adaptation of the extended multiplicative signal correction (EMSC) algorithm described by Martens and Stark – which draws on some prior knowledge of what the expected signal should look like and corrects for unintended scattering effects [45]. It also builds on an earlier Mie scattering modification of the EMSC that accounts for the Mie scattering effects in single cell spectra from synchrotron microscopy [46]. The fundamentals of the RMieS-EMSC algorithm are described in [47]. The algorithm was later updated to employ an iterative approach applying the full Mie scattering theory [44]. This updated algorithm, without the GPU computing adaptation that was used in the paper, was applied to the cell spectra discussed earlier. Although, the initial algorithm was developed for single cell spectral

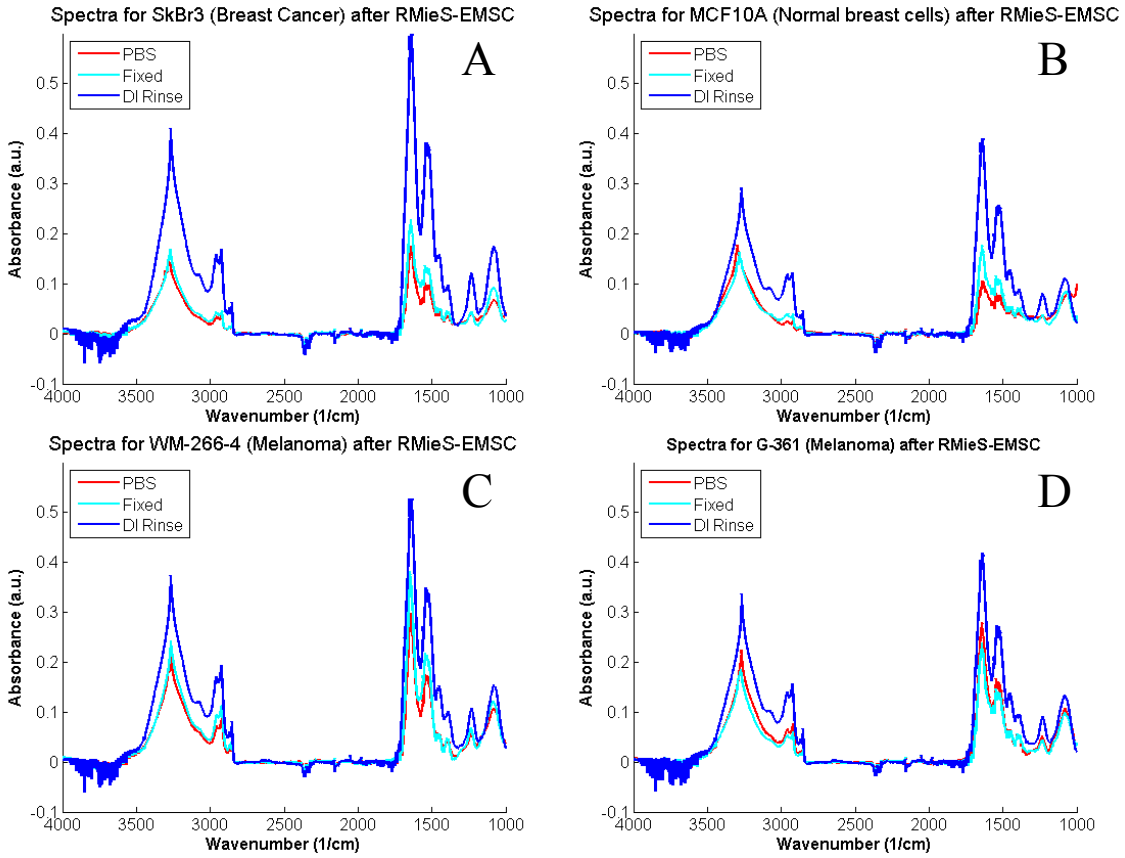

Figure 10. Spectra comparing sample preparations after using ther RMieS-EMSC algorithm. The removal of scattering distortion clearly removes background signal and enables the peaks in the fingerprint region to be more easily seen

measurements, it has also been applied to tissue samples and should also be applicable to a layer of cells [44, 46],[48].

Like the EMSC algorithm, the RMieS-EMSC requires a reference spectrum; however, the algorithm can work for most biological samples using a single reference spectrum of a thin film of Matrigel. Bassan et al. have shown that as long as the reference spectrum is somewhat close to the expected spectrum it can remove the scattering

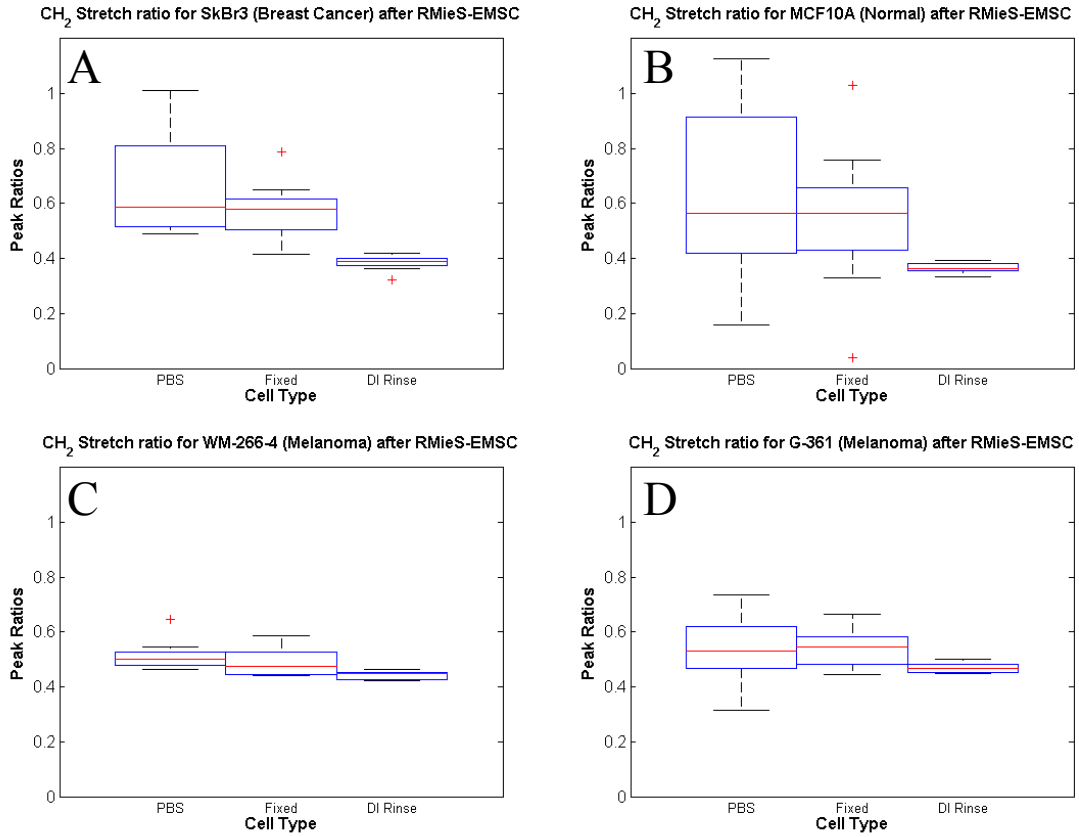

Figure 11. Comparison of sample preparation using the RMieS-EMSC algorithm on the symmetric vs anti-symmetric CH2 stretch ratio. (A) the DI rinse prepration was significantly lower than the other two methods ($p < 0.005$). (C) The DI rinse was also lower than the PBS preparation in the WM-266-4 cell line. (B) and (D) the were no significant differences between the methods

distortion; they showed this by using three different reference spectra to obtain the same spectrum after correction. The same paper demonstrated that it takes between 20-30 iterations of the correction algorithm to remove the vast majority of scattering distortion as well as the influence of the reference spectra [48]. The number of iterations depends on the similarity of the spectra, to account for any issues in spectra quality 50 iterations were run to be on the safe side and not have any influence from the reference spectra.

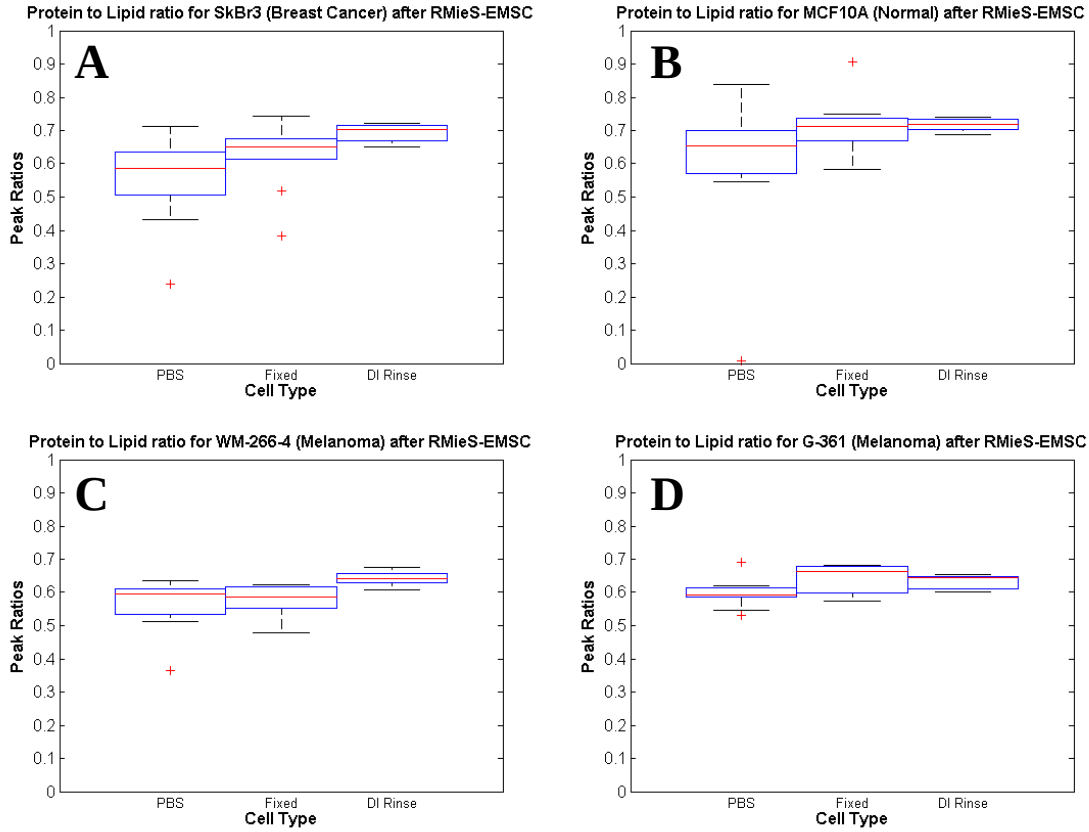

Figure 12. Comparison of sample preparation using the RMieS-EMSC algorithm on the protein to lipid stretch ratio. For the SkBr3 (A) and WM-266-4 (C) cell lines the DI rinse was larger than the PBS dried sample ($p < 0.01$). No differences were significant in the MCF10A line (B), and in the G-361 cell line the fixed sample was larger than the PBS dried sample.

4.1. Sample Preparations after RMieS-EMSC

The sample correction algorithm had a large effect on the FTIR spectra as seen from figure 10. The major differences are the sharpening of the O-H stretching peak around 3300 along with the flattening of the region between ~2800 cm^{-1} to 1700 cm^{-1}, and removal of scattering between 1500 and 1000 cm^{-1}. A close of up this region is included in Appendix A figure 19. The effect on the biomarkers was less clear and was

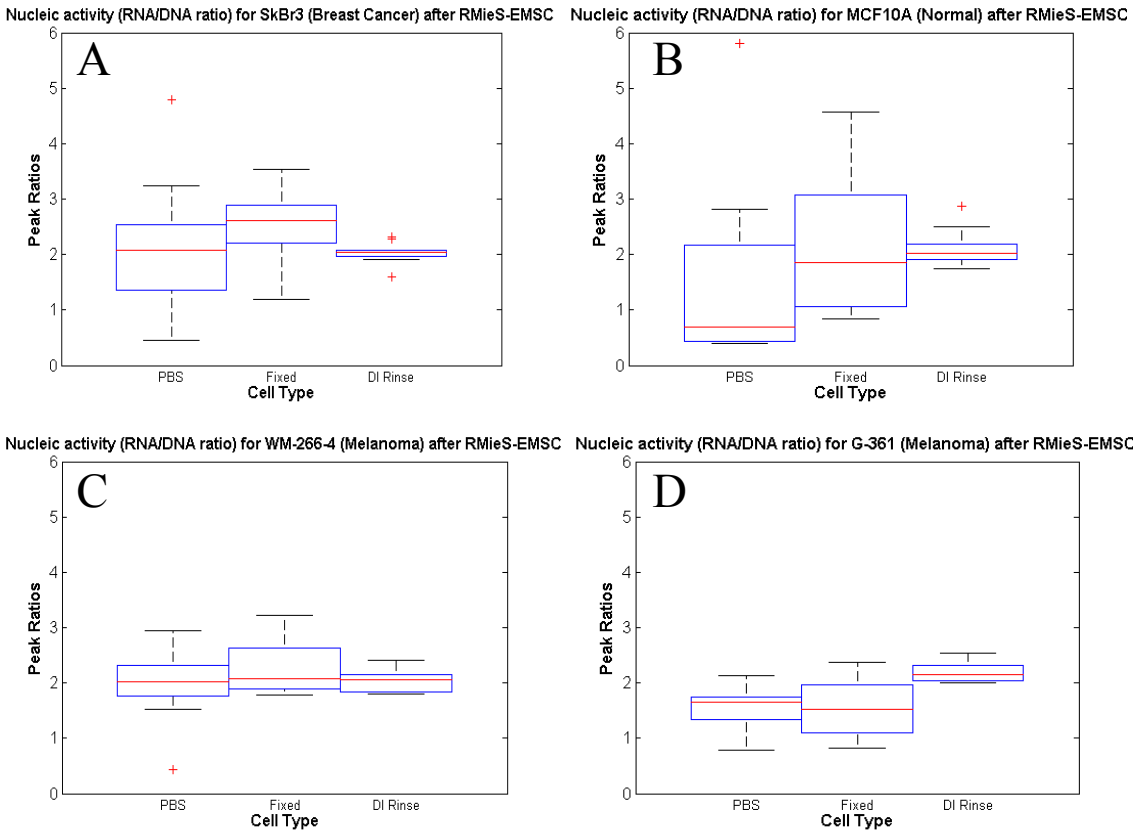

Figure 13. Comparison of sample preparation using the RMieS-EMSC algorithm on the nucleic activity biomarker. For three of the cell lines (A,B, and C) there were not differences between sample preparation methods, however in the G-361 cell line (D) the DI rinse was significantly larger than the PBS sample ($p < 0.005$).

not consistent across cell lines, but this could also be due to different amounts of scattering distortion in the original spectra. The MCF10A cell line lost all significant differences between the sample preparations, while the other three cell lines both gained some significant differences and lost some. For the CH_2 stretch ratio (figure 11) the correction algorithm shifted the PBS and fixed samples closer, resulting in the DI rinse ratio becoming significantly smaller than both PBS and fixed samples for the SkBr3 line ($p < 0.005$), but only the PBS for the WM-266-4 ($p < 0.005$). One big change from the

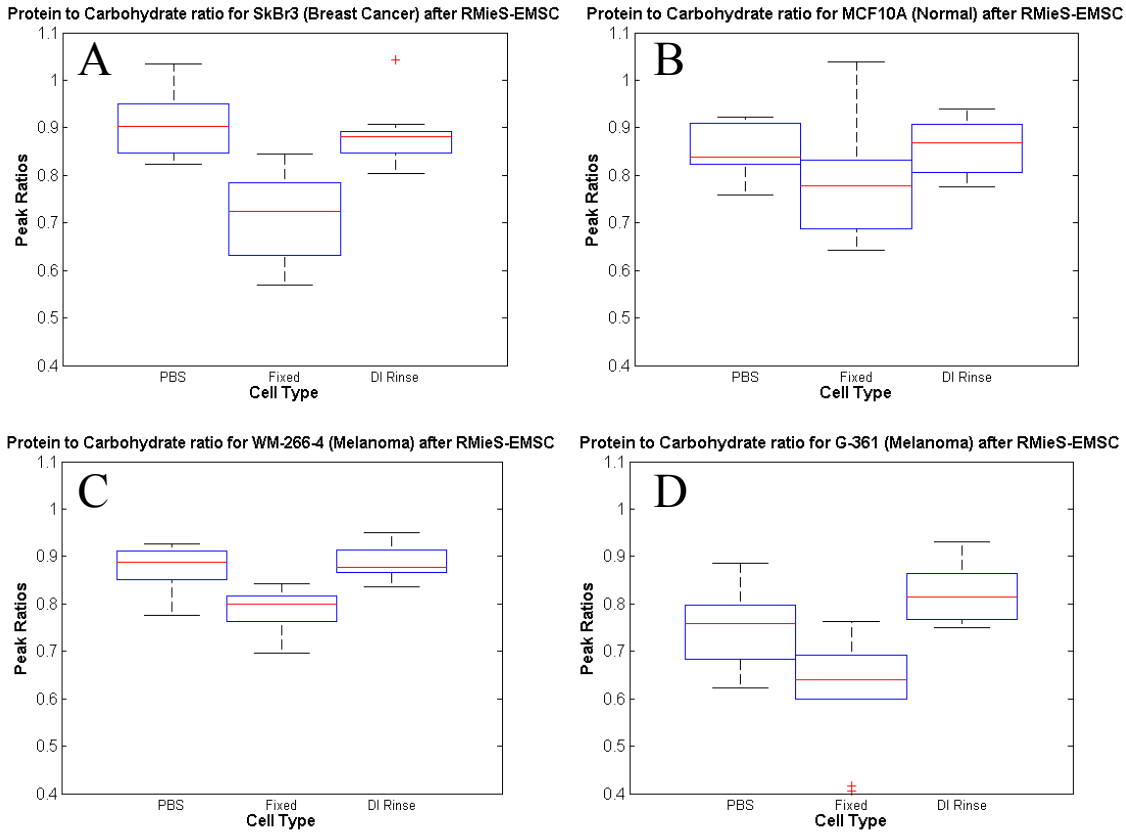

Figure 14. Comparison of sample preparation using the RMieS-EMSC algorithm on the protein to carbohydrate ratio. For all cell lines except the MCF10A (B) the fixed samples had significantly smaller ratios than either the PBS or DI rinsed samples ($p < 0.05$).

correction algorithm is that 3 cell lines – all but the MCF10A line – had significant differences for the protein to lipid ratio (figure 12) where there were no differences before. For the SkBr3 and WM-266-4 cell lines the DI rinse was larger than the PBS, ($p < 0.01$) and for the G-361 the fixed sample was larger than the PBS ($p < 0.05$). Only the G-361 cell line had any difference in the nucleic activity biomarker (figure 13), with a DI rinse ratio than the PBS sample ($p < 0.005$). The protein to carbohydrate ratio was lower in the fixed sample than both the PBS and DI rinse ($p < 0.05$) for all but the MCF10A

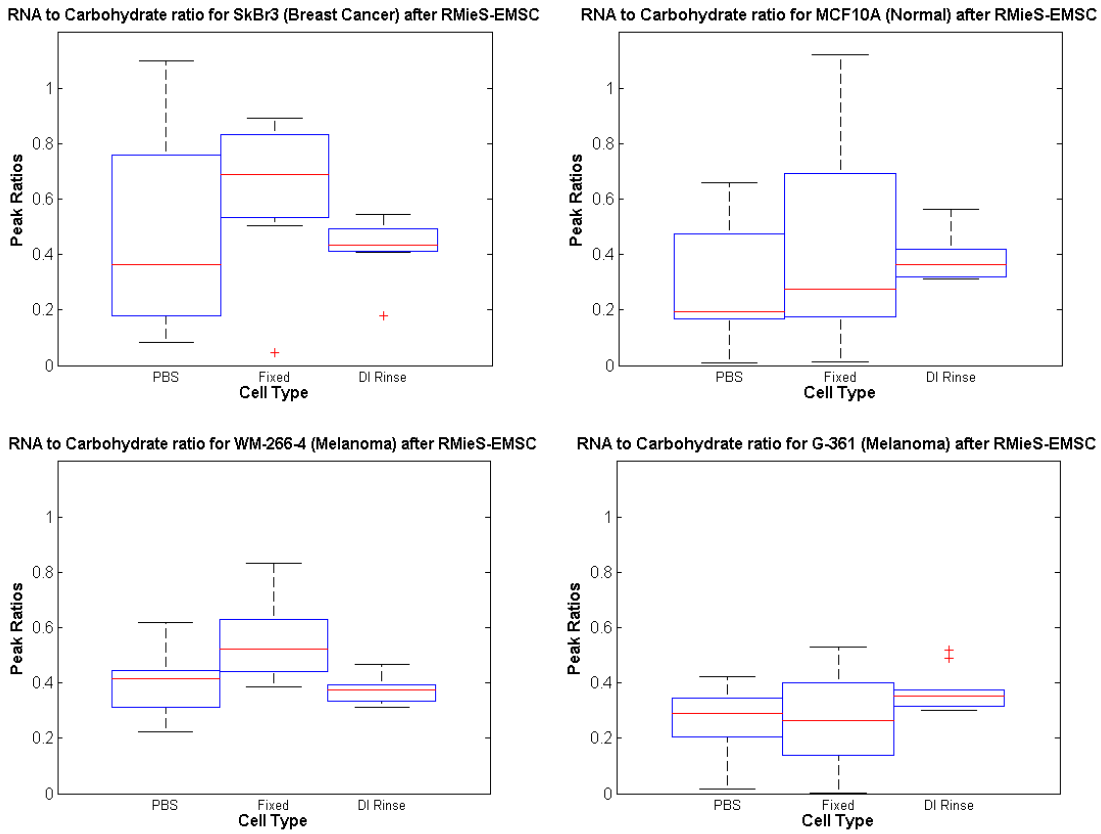

Figure 15 Comparison of sample preparation using the RMieS-EMSC algorithm on the RNA to carbohydrate ratio. For all cell lines except the WM-266-4 (C) there were no differences in the sample preparations. In the WM-266-4 cell line the fixed sample had the highest ratio ($p < 0.05$).

cell line (figure 14). For the RNA to carbohydrate ratio (figure 15) the only significant difference between the sample preparations was in the WM-266-4 cell line, in which the sample dried in Cytofix had a larger ratio than both of the other methods ($p < 0.05$)

4.2. Cell Line Comparison after RMieS-EMSC

The Smart iTR with the low resolution setting already had very little scattering distortion above 1700 cm^{-1}, but the fingerprint region had some distortion leading to a

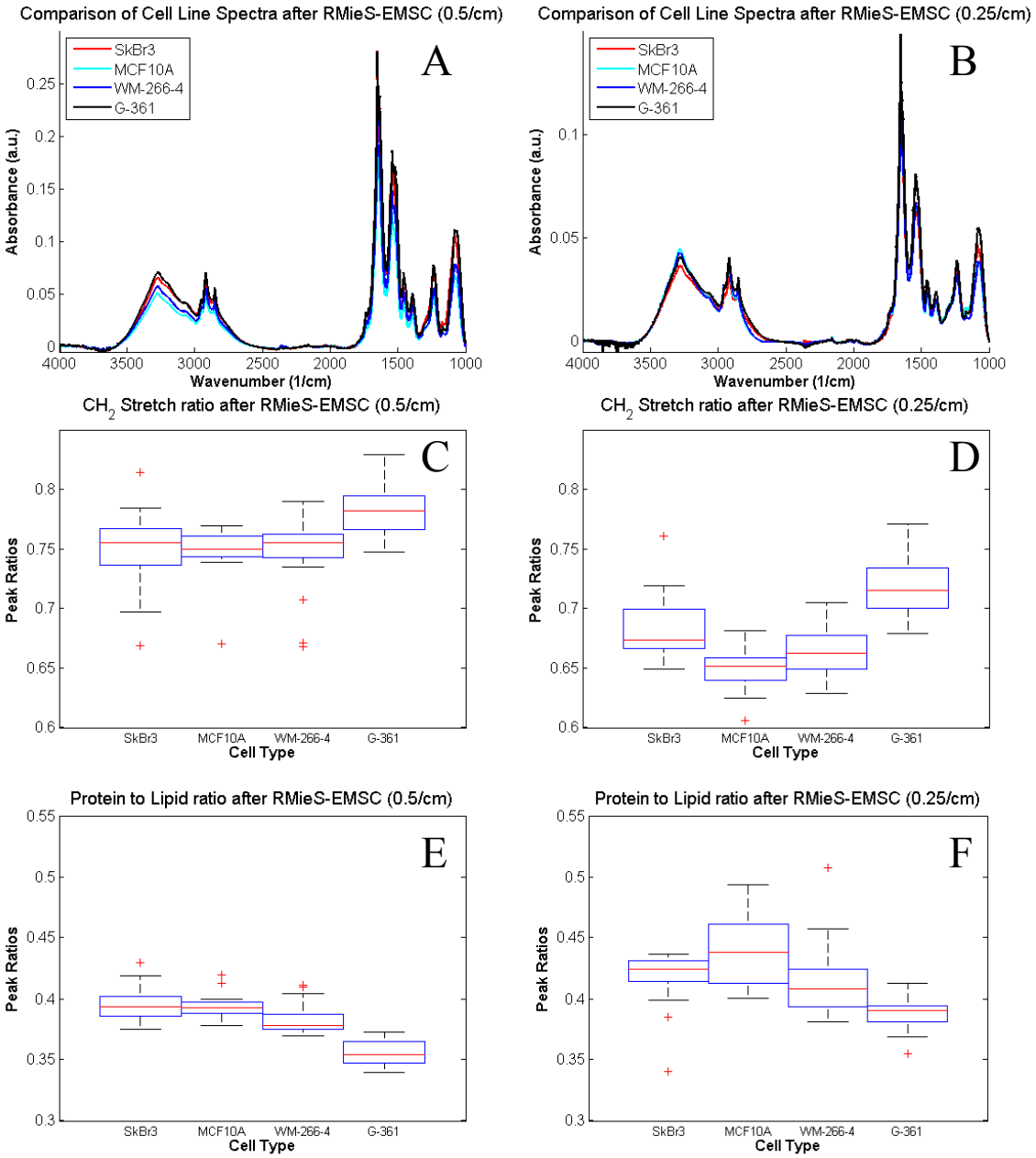

Figure 16. ATR spectra from all 4 cell lines using the DI rinsed samples at 0.5 cm^{-1} (A) and at 0.25 cm^{-1} (B) after the RMieS-EMSC algorithm. For the CH_2 stretch ratio at 0.5 cm^{-1} (C) and 0.25 cm^{-1} (D) the G-361 cell line was significantly larger than the other cell lines ($p < 0.005$), however, in addition for the 0.25 cm^{-1} run the SkBr3 cell line was larger than the MCF10A line ($p < 0.001$). The G-361 cell line was the lowest of all cell lines ($p < 0.001$) in both the 0.5 cm^{-1} (E) and 0.25 cm^{-1} runs (F) for the protein to lipid ratio. The runs were not identical because in the 0.5 cm^{-1} run the WM-266-4 cell line was lower than the SkBr3 and MCF10A cell lines ($p < 0.05$) but for 0.25 cm^{-1} (F) the MCF10A cell line was the largest ($p < 0.05$).

high baseline. The RMieS-EMSC algorithm had only a small effect above 1700 cm^{-1} but removed the distortion from the fingerprint region (figure 16A). The higher resolution spectra had much more scattering distortion in the signal, but once corrected has a very similar shape to the lower resolution spectra (figure 16B).

Again, after applying the correction algorithm some of the differences between cell lines changed, either losing significance or becoming significant. As before with the Smart iTR attachment, both runs had similarities between the ratios which were different for most of the biomarkers analyzed. The G-361 cell line had a larger CH_2 symmetric to anti-symmetric ratio than any other cell line ($p < 0.005$) and this was true in both runs (figure 16 C and D), with the only difference being a smaller MCF10A ratio than SkBr3 in the high resolution run ($p < 0.001$). The low resolution lost all significant differences for the other cell line from the uncorrected spectra. For the protein to lipid ratio (figure 16E and F) the G-361 had the lowest ratio of all cell lines ($p <0.005$), and MCF10A had a higher ratio than WM-266-4 ($p < 0.05$) in both runs. However, there were two differences that were unique to each run. For the nucleic activity (figures 17A and B) both of the melanoma cell lines were different from the breast cancer lines in both runs ($p < 0.01$), but for the lower resolution run all the cell lines were different ($p < 0.01$). The only biomarker where a large difference was seen between the runs was the protein to carbohydrate ratio. There were no differences in the high resolution run (figure 17D) whereas in the low resolution run (figure 17C) both melanoma cell lines had higher ratios than the breast cell lines ($p < 0.01$). For the RNA to carbohydrate ratio (figures 17E and F) the runs were very similar with the SkBr3 cell line having the highest ratio ($p < 0.001$), and MCF10A cell line larger than the WM-266-4 cell line ($p < 0.01$), and in the lower

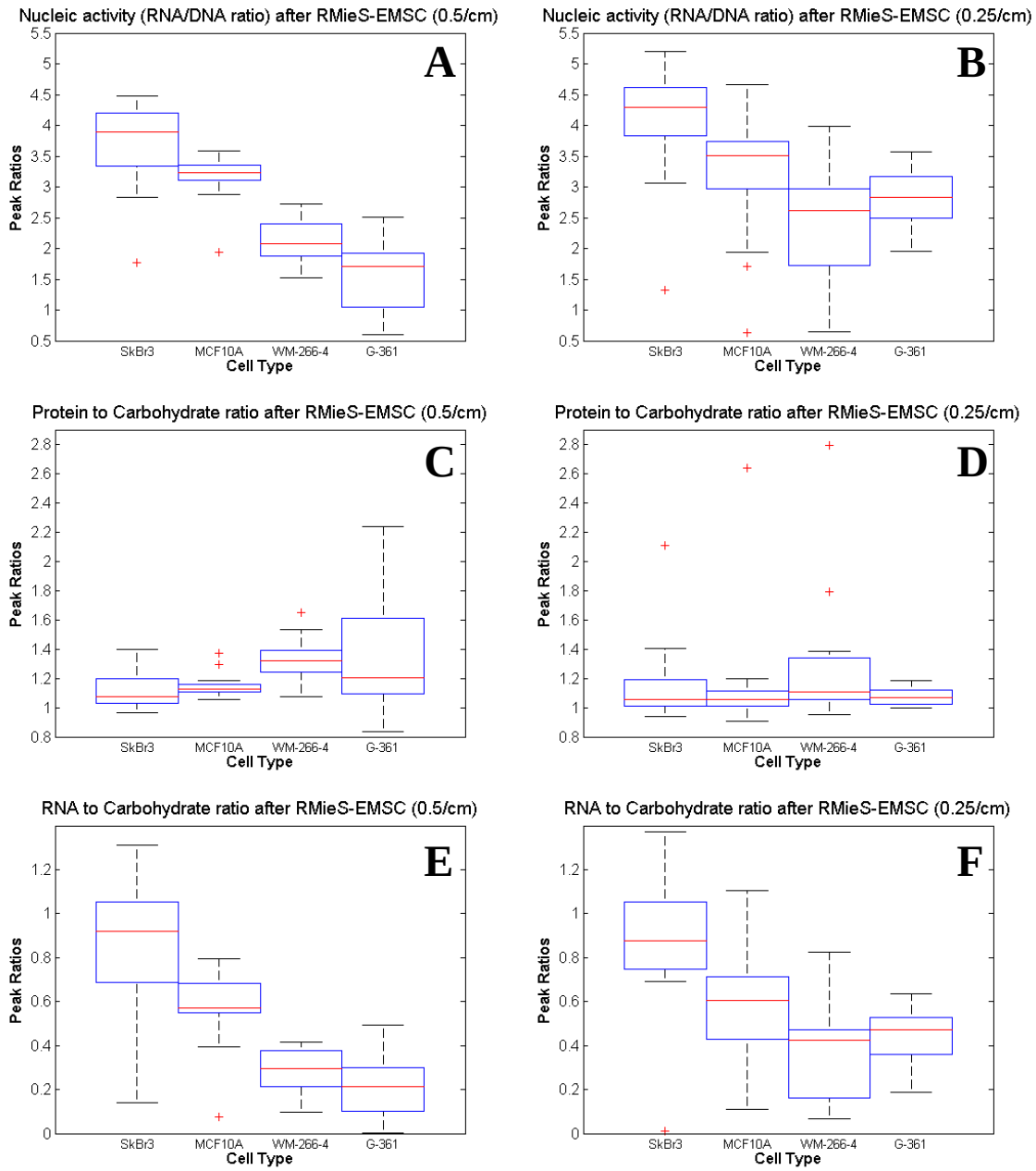

Figure 17. Biomarkers after RMieS-EMSC. Nucleic activity biomarker for 0.5 cm^{-1}, (A) all cell lines are significantly different ($p < 0.01$) and for 0.25 cm^{-1} (B) the melanoma cell lines had smaller ratios than the breast cell lines ($p < 0.01$). In the protein to carbohydrate ratio 0.5 cm^{-1} (C) the breast cells lines were different from the melanoma cell lines ($p < 0.05$) and for 0.25 cm^{-1} (D) there were no differences between the cell lines. For the RNA to carbohydrate ratio in both the 0.5 cm^{-1} (E) and 0.25 cm^{-1} (F) runs the SkBr3 cell line was the largest ($p <0.001$) and the MCF10A cell line was larger than the WM-266-4 cell line ($p <.0.001$). Yet, in the 0.5 cm^{-1} (E) run, the MCF10A cell line was also larger than G-361 ($p < 0.001$).

resolution run, it was also larger than the G-361 cell line ($p < 0.001$).

When the runs were combined, the significant differences between cell lines were the common differences that both corrected cell lines had plus a few additional differences. There were only three significant differences between cell lines that were not different in both of the runs: the lower ratio of the G-361 cell line from the MCF10A in the nucleic activity biomarker ($p < 0.001$), the higher protein to carbohydrate ratio in the WM-266-4 cell line compared to the SkBr3 cell line, and the larger ratio of RNA to carbohydrates in the MCF10A cell line compared to the G-361 cell line.

These differences from the uncorrected spectra demonstrate how scattering can alter the spectra in ways that could affect cancer detection. Before the RMieS-EMSC the high resolution run only had biomarker that showed any difference between the breast cancer cell line and normal breast cell line, after correction there were four biomarkers that were significantly different. However, in the lower resolution run, only two of the three biomarkers remained different after correction, and neither of the other biomarkers had any difference between the two cell lines. The markers do a better job at distinguishing between melanoma cell and breast cancer or normal breast cells. In the lower resolution run the G-361 cell line was different from both breast cell lines in all biomarkers, and the WM-266-4 was different in all but the CH_2 stretch. The high resolution run had the same result for the WM-266-4 cell line, but G-361 different from SkBr3 in four biomarkers, but from MCF10A in only two.

Despite the visual similarities of the low resolution spectra to the corrected spectra, aside from the nucleic activity and RNA to carbohydrate biomarkers, all of the

other biomarkers experienced some cell line ratios changing in relation to each other. This means that scattering distortion could either hide or create differences that may not be present between cell lines, even in spectra with relatively little scattering distortion.

Chapter 5

Conclusions

This paper demonstrates that the method of sample preparation can induce significant spectral changes when dealing with biological samples. The research also suggests that the sampling collecting modules and experimental settings can also affect the spectra shape, but more research is needed to confirm this. After applying the RMieS-EMSC algorithm the spectra from all cases looked more similar, but the large peak at 3300 cm^{-1} in the GoldenGate ATR spectra still stands out from the spectra taken with the Smart iTR. This paper also found that when using simple cancer detection methods based on peak ratios it is critical to maintain identical sampling conditions, and it may not be possible to use detection methods from other cancer cell lines. Even using detection methods with a different sample preparation than it was initially used with could cause problems with diagnosis. The cancer biomarkers tested in this paper for the breast cancer and melanoma cell lines were not consistently different, and even in the cases where the means were different, there was still some overlap in the sample ratios, suggesting that it

would be a poor predictor of cancer. However, these biomarkers were not designed to identify breast cancer, so it is possible that the changes in breast cancer are different from the changes in the cancers these biomarkers were found to detect.

Many of the papers doing cancer detection using FTIR spectra rely on a number of small differences between the cell or tissue spectra. It is the opinion of the author that many of the cancer detection techniques described in the literature may not be effective when used with different sample preparations or even for determining the cancer status of a different cancer type. The FTIR spectra of cell and tissue samples can be used to detect slight differences between normal and cancerous or even pre-cancerous cells, but these minute differences may be hidden by changes from other factors. In the research presented the cell lines did not respond identically to the changes in sample preparation, which could have to do with cell properties other than whether or not a cell is cancerous. This will complicate attempts to compare results using different sample preparations.

The conclusion from this research is that despite the differences between cancerous and normal cells, using FTIR for determining cancer status is a difficult problem to solve and will likely remain in research labs for the near future. However, with improvements in MIR sources and detectors, it is possible that these will enable better sampling conditions to allow for more reliable detection.

References

[1] R. Siegel, D. Naishadham, and A. Jemal, "Cancer Statistics, 2012," *Ca-a Cancer Journal for Clinicians,* vol. 62, pp. 10-29, Jan-Feb 2012.

[2] M. Heron, "Deaths: Leading Causes for 2007," *National Vital Statistics Reports: vol 59, no 8. Hyattsville, MD: National Center for Health Statistics,* 2011.

[3] S. L. Murphy, J. Xu, and M. A. Kochanek, "Deaths: Preliminary Data for 2010," *National Vital Statistics Reports: vol 60, no 4. Hyattsville, MD: National Center for Health Statistics,* 2012.

[4] E. Bogomolny, S. Argov, S. Mordechai, and M. Huleihel, "Monitoring of viral cancer progression using FTIR microscopy: A comparative study of intact cells and tissues," *Biochimica Et Biophysica Acta-General Subjects,* vol. 1780, pp. 1038-1046, Sep 2008.

[5] USPTF, "Screening for Skin Cancer: U.S. Preventive Services Task Force Recommendation Statement," *Annals of Internal Medicine,* vol. 150, pp. 188-193, 2009.

[6] A. Bleyer and R. Barr, "Cancer in Young Adults 20 to 39 Years of Age: Overview," *Seminars in Oncology,* vol. 36, pp. 194-206, Jun 2009.

[7] D. J. Rhodes, C. B. Hruska, S. W. Phillips, D. H. Whaley, and M. K. O'Connor, "Dedicated Dual-Head Gamma Imaging for Breast Cancer Screening in Women with Mammographically Dense Breasts," *Radiology,* vol. 258, pp. 106-118, Jan 2011.

[8] E. Bogomolny, M. Huleihel, A. Salman, A. Zwielly, R. Moreh, and S. Mordechai, "Attenuated total reflectance spectroscopy: a promising technique for early detection of premalignancy," *Analyst,* vol. 135, pp. 1934-1940, 2010.

[9] L. R. Bickford, G. Agollah, R. Drezek, and T. K. Yu, "Silica-gold nanoshells as potential intraoperative molecular probes for HER2-overexpression in ex vivo breast tissue using near-infrared reflectance confocal microscopy," *Breast Cancer Research and Treatment,* vol. 120, pp. 547-555, Apr 2010.

[10] A. Luini, J. Rososchansky, G. Gatti, S. Zurrida, P. Caldarella, G. Viale, G. R. dos Santos, and A. Frasson, "The surgical margin status after breast-conserving surgery: discussion of an open issue," *Breast Cancer Research and Treatment,* vol. 113, pp. 397-402, Jan 2009.

[11] B. Fisher, S. Anderson, J. Bryant, R. G. Margolese, M. Deutsch, E. R. Fisher, J. Jeong, and N. Wolmark, "Twenty-year follow-up of a randomized trial comparing

total mastectomy, lumpectomy, and lumpectomy plus irradiation for the treatment of invasive breast cancer," *New England Journal of Medicine,* vol. 347, pp. 1233-1241, Oct 17 2002.

[12] N. Q. Mirza, G. Vlastos, F. Meric, T. A. Buchholz, N. Esnaola, S. E. Singletary, H. M. Kuerer, L. A. Newman, F. C. Ames, M. I. Ross, B. W. Feig, R. E. Pollock, M. McNeese, E. Strom, and K. K. Hunt, "Predictors of locoregional recurrence among patients with early-stage breast cancer treated with breast-conserving therapy," *Annals of Surgical Oncology,* vol. 9, pp. 256-265, Apr 2002.

[13] K. P. McGuire, A. A. Santillan, P. Kaur, T. Meade, J. Parbhoo, M. Mathias, C. Shamehdi, M. Davis, D. Ramos, and C. E. Cox, "Are Mastectomies on the Rise? A 13-Year Trend Analysis of the Selection of Mastectomy Versus Breast Conservation Therapy in 5865 Patients," *Annals of Surgical Oncology,* vol. 16, pp. 2682-2690, Oct 2009.

[14] C. Dener, A. Inan, M. Sen, and S. Demirci, "Intraoperative Frozen Section for Margin Assessment in Breast Conserving Surgery," *Scandinavian Journal of Surgery,* vol. 98, pp. 34-40, 2009.

[15] A. C. Barros, M. Pinotti, L. C. Teixeira, M. D. Ricci, and J. A. Pinotti, "Outcome analysis of patients with early infiltrating breast carcinoma treated by surgery with intraoperative evaluation of surgical margins," *Tumori,* vol. 90, pp. 592-595, Nov-Dec 2004.

[16] E. Weinberg, C. Cox, E. Dupont, L. White, M. Ebert, H. Greenberg, N. Diaz, V. Vercel, B. Centeno, A. Cantor, and S. Nicosia, "Local recurrence in lumpectomy patients after imprint cytology margin evaluation," *American Journal of Surgery,* vol. 188, pp. 349-354, Oct 2004.

[17] R. Bhargava, "Towards a practical Fourier transform infrared chemical imaging protocol for cancer histopathology," *Analytical and Bioanalytical Chemistry,* vol. 389, pp. 1155-1169, Oct 2007.

[18] S. van den Driesche, W. Witarski, S. Pastorekova, H. Breiteneder, C. Hafner, and M. J. Vellekoop, "A label-free indicator for tumor cells based on the CH(2)-stretch ratio," *Analyst,* vol. 136, pp. 2397-2402, 2011.

[19] K. B. Reed, J. D. Brewer, C. M. Lohse, K. E. Bringe, C. N. Pruitt, and L. E. Gibson, "Increasing Incidence of Melanoma Among Young Adults: An Epidemiological Study in Olmsted County, Minnesota," *Mayo Clinic Proceedings,* vol. 87, pp. 328-334, 2012.

[20] NCI, "A Snapshot of Melanoma," National Cancer Institute: U.S. Department of Health and Human Services, National Institute of Health. Accessed from http://www.cancer.gov/aboutnci/servingpeople/cancer-statistics/snapshots 2011.

[21] M. P. Purdue, L. E. B. Freeman, W. F. Anderson, and M. A. Tucker, "Recent Trends in Incidence of Cutaneous Melanoma among US Caucasian Young Adults," *Journal of Investigative Dermatology,* vol. 128, pp. 2905-3908, Dec 2008.

[22] K. A. Freedberg, A. C. Geller, D. R. Miller, R. A. Lew, and H. K. Koh, "Screening for malignant melanoma: A cost-effectiveness analysis," *Journal of the American Academy of Dermatology,* vol. 41, pp. 738-745, Nov 1999.

[23] P. Carli, V. de Giorgi, A. Chiarugi, P. Nardini, M. A. Weinstock, E. Crocetti, M. Stante, and B. Giannotti, "Addition of dermoscopy to conventional naked-eye examination in melanoma screening: A randomized study," *Journal of the American Academy of Dermatology,* vol. 50, pp. 683-689, May 2004.

[24] G. Zonios, A. Dimou, I. Bassukas, D. Galaris, A. Tsolakidis, and E. Kaxiras, "Melanin absorption spectroscopy: new method for noninvasive skin investigation and melanoma detection," *Journal of Biomedical Optics,* vol. 13, Jan-Feb 2008.

[25] H. Lorentzen, K. Weismann, C. S. Petersen, F. G. Larsen, L. Secher, and V. Skodt, "Clinical and dermatoscopic diagnosis of malignant melanoma - Assessed by expert and non-expert groups," *Acta Dermato-Venereologica,* vol. 79, pp. 301-304, Jul 1999.

[26] L. B. Mostaco-Guidolin, L. S. Murakami, M. R. Batistuti, A. Nomizo, and L. Bachmann, "Molecular and chemical characterization by Fourier transform infrared spectroscopy of human breast cancer cells with estrogen receptor expressed and not expressed," *Spectroscopy-an International Journal,* vol. 24, pp. 501-510, 2010.

[27] P. Bassan, H. J. Byrne, J. Lee, F. Bonnier, C. Clarke, P. Dumas, E. Gazi, M. D. Brown, N. W. Clarke, and P. Gardner, "Reflection contributions to the dispersion artefact in FTIR spectra of single biological cells," *Analyst,* vol. 134, pp. 1171-1175, 2009.

[28] J. Lee, E. Gazi, J. Dwyer, M. D. Brown, N. W. Clarke, J. M. Nicholson, and P. Gardner, "Optical artefacts in transflection mode FTIR microspectroscopic images of single cells on a biological support: the effect of back-scattering into collection optics," *Analyst,* vol. 132, pp. 750-755, 2007.

[29] J. Anastassopoulou, E. Boukaki, C. Conti, P. Ferraris, E. Giorgini, C. Rubini, S. Sabbatini, T. Theophanides, and G. Tosi, "Microimaging FT-IR spectroscopy on pathological breast tissues," *Vibrational Spectroscopy,* vol. 51, pp. 270-275, Nov 10 2009.

[30] H. Fabian, P. Lasch, M. Boese, and W. Haensch, "Mid-IR microspectroscopic Imaging of breast tumor tissue sections," *Biopolymers,* vol. 67, pp. 354-357, 2002.

[31] W. G. Jiang, T. A. Martin, and R. E. Mansel, "Molecular detection of micro-metastasis in breast cancer," *Critical Reviews in Oncology Hematology,* vol. 43, pp. 13-31, Jul 2002.

[32] F. L. Martin, J. G. Kelly, V. Llabjani, P. L. Martin-Hirsch, I. I. Patel, J. Trevisan, N. J. Fullwood, and M. J. Walsh, "Distinguishing cell types or populations based on the computational analysis of their infrared spectra," *Nature Protocols,* vol. 5, pp. 1748-1760, 2010.

[33] B. Bird, K. Bedrossian, N. Laver, M. Miljkovic, M. J. Romeo, and M. Diem, "Detection of breast micro-metastases in axillary lymph nodes by infrared micro-spectral imaging," *Analyst,* vol. 134, pp. 1067-1076, 2009.

[34] R. Bhargava and I. W. Levin, "Fourier transform infrared imaging: Theory and practice," *Analytical Chemistry,* vol. 73, pp. 5157-5167, Nov 1 2001.

[35] E. Gazi, J. Dwyer, N. P. Lockyer, J. Miyan, P. Gardner, C. Hart, M. Brown, and N. W. Clarke, "Fixation protocols for subcellular imaging by synchrotron-based Fourier transform infrared microspectroscopy," *Biopolymers,* vol. 77, pp. 18-30, Jan 2005.

[36] M. J. Nasse, M. J. Walsh, E. C. Mattson, R. Reininger, A. Kajdacsy-Balla, V. Macias, R. Bhargava, and C. J. Hirschmugl, "High-resolution Fourier-transform infrared chemical imaging with multiple synchrotron beams," *Nature Methods,* vol. 8, pp. 413-U58, May 2011.

[37] C. A. Simmons, J. Zilberberg, and P. F. Davies, "A rapid, reliable method to isolate high quality endothelial RNA from small spatially-defined locations," *Annals of Biomedical Engineering,* vol. 32, pp. 1453-1459, Oct 2004.

[38] R. K. Sahu, S. Argov, A. Salman, U. Zelig, M. Huleihel, N. Grossman, J. Gopas, J. Kapelushnik, and S. Mordechai, "Can Fourier transform infrared spectroscopy at higher wavenumbers (mid IR) shed light on biomarkers for carcinogenesis in tissues?," *Journal of Biomedical Optics,* vol. 10, Sep-Oct 2005.

[39] A. I. Mazur, E. J. Marcsisin, B. Bird, M. Miljkovic, and M. Diem, "Evaluating Different Fixation Protocols for Spectral Cytopathology, Part 2: Cultured Cells," *Analytical Chemistry,* vol. 84, pp. 8265-8271, Oct 2 2012.

[40] E. Gazi, J. Dwyer, N. P. Lockyer, P. Gardner, J. H. Shanks, J. Roulson, C. A. Hart, N. W. Clarke, and M. D. Brown, "Biomolecular profiling of metastatic prostate cancer cells in bone marrow tissue using FTIR microspectroscopy: a pilot

study," *Analytical and Bioanalytical Chemistry,* vol. 387, pp. 1621-1631, Mar 2007.

[41] E. J. Hwang, Lee, S.K., "Live Cells detection in breast cell-line by FTIR micro-spectrometer," in *IEEE SENSORS* 2008.

[42] E. J. Marcsisin, "Infrared spectroscopy to monitor drug response of individual live cells," in *Chemistry Dissertations*: Paper 36., 2011.

[43] C. Petibois, M. Cestelli-Guidi, M. Piccinini, M. Moenner, and A. Marcelli, "Synchrotron radiation FTIR imaging in minutes: a first step towards real-time cell imaging," *Analytical and Bioanalytical Chemistry,* vol. 397, pp. 2123-2129, Jul 2010.

[44] P. Bassan, A. Kohler, H. Martens, J. Lee, H. J. Byrne, P. Dumas, E. Gazi, M. Brown, N. Clarke, and P. Gardner, "Resonant Mie Scattering (RMieS) correction of infrared spectra from highly scattering biological samples," *Analyst,* vol. 135, pp. 268-277, 2010.

[45] H. Martens and E. Stark, "Extended Multiplicative Signal Correction and Spectral Interference Subtraction - New Preprocessing Methods for near-Infrared Spectroscopy," *Journal of Pharmaceutical and Biomedical Analysis,* vol. 9, pp. 625-635, 1991.

[46] A. Kohler, J. Sule-Suso, G. D. Sockalingum, M. Tobin, F. Bahrami, Y. Yang, J. Pijanka, P. Dumas, M. Cotte, D. G. van Pittius, G. Parkes, and H. Martens, "Estimating and correcting Mie scattering in synchrotron-based microscopic Fourier transform infrared spectra by extended multiplicative signal correction," *Applied Spectroscopy,* vol. 62, pp. 259-266, Mar 2008.

[47] P. Bassan, H. J. Byrne, F. Bonnier, J. Lee, P. Dumas, and P. Gardner, "Resonant Mie scattering in infrared spectroscopy of biological materials - understanding the 'dispersion artefact'," *Analyst,* vol. 134, pp. 1586-1593, 2009.

[48] P. Bassan, A. Sachdeva, A. Kohler, C. Hughes, A. Henderson, J. Boyle, J. H. Shanks, M. Brown, N. W. Clarke, and P. Gardner, "FTIR microscopy of biological cells and tissue: data analysis using resonant Mie scattering (RMieS) EMSC algorithm," *Analyst,* vol. 137, pp. 1370-1377, 2012.

Appendix A

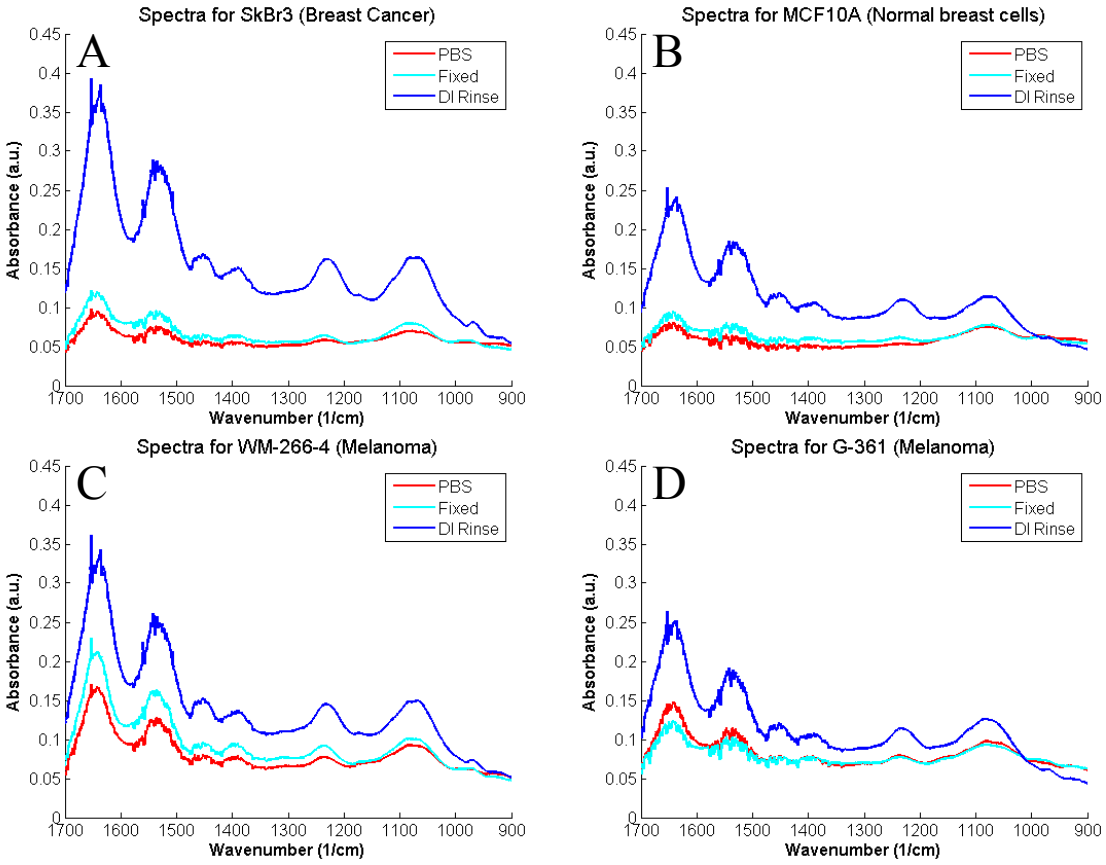

Figure 18. Fingerprint region spectral comparison of sample preparations. The difference between the DI rinse and the other preparations is apparent from the much larger peak heights of the DI rinse in the fingerprint region. The differences between sample preparations are most clearly seen in the breast cell lines (A and B), while the melanomal cell lines only show a slight to moderate improvement (C and D)

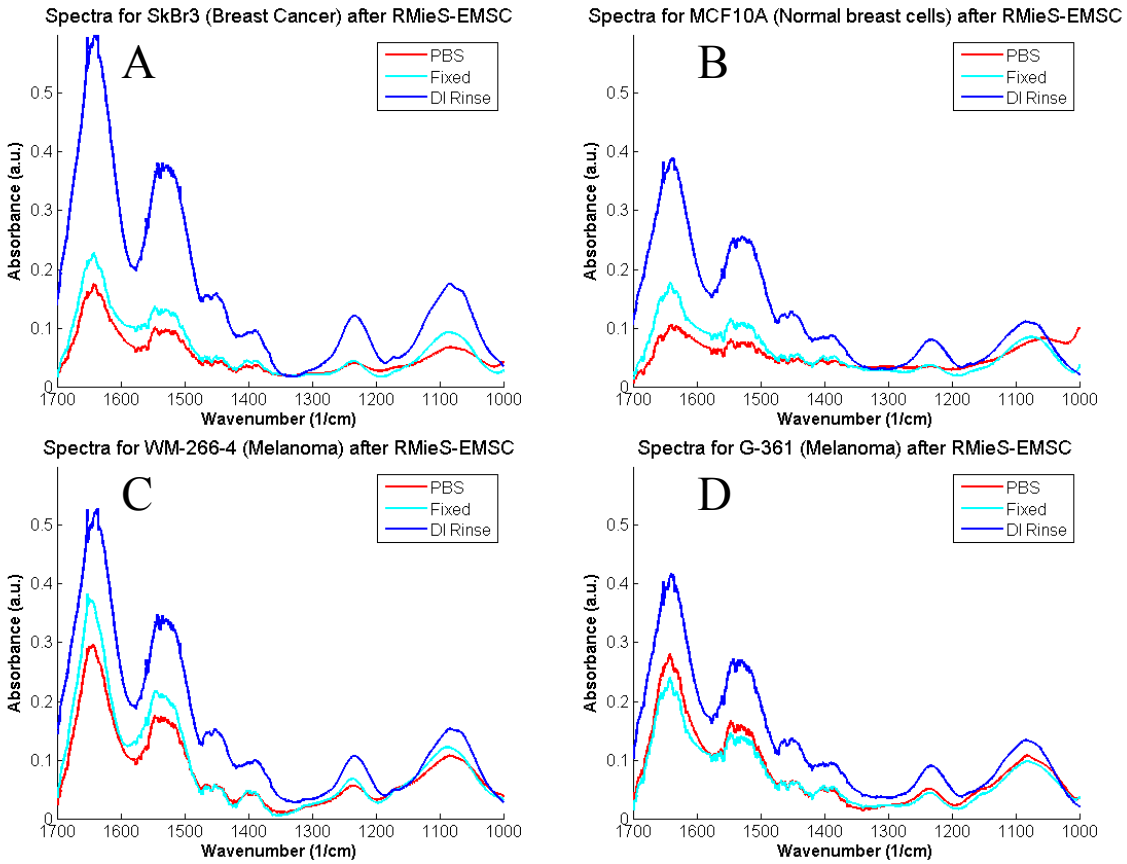

Figure 19. Fingerprint region spectral comparison of sample preparations after RMieS-EMSC. By removing the excess scattering from the signal in the breast cell lines, it is easier to see the peaks (A and B). This same improvement is seen in the melanoma cell lines making the PBS and fixed sample preparations look better (C and D).

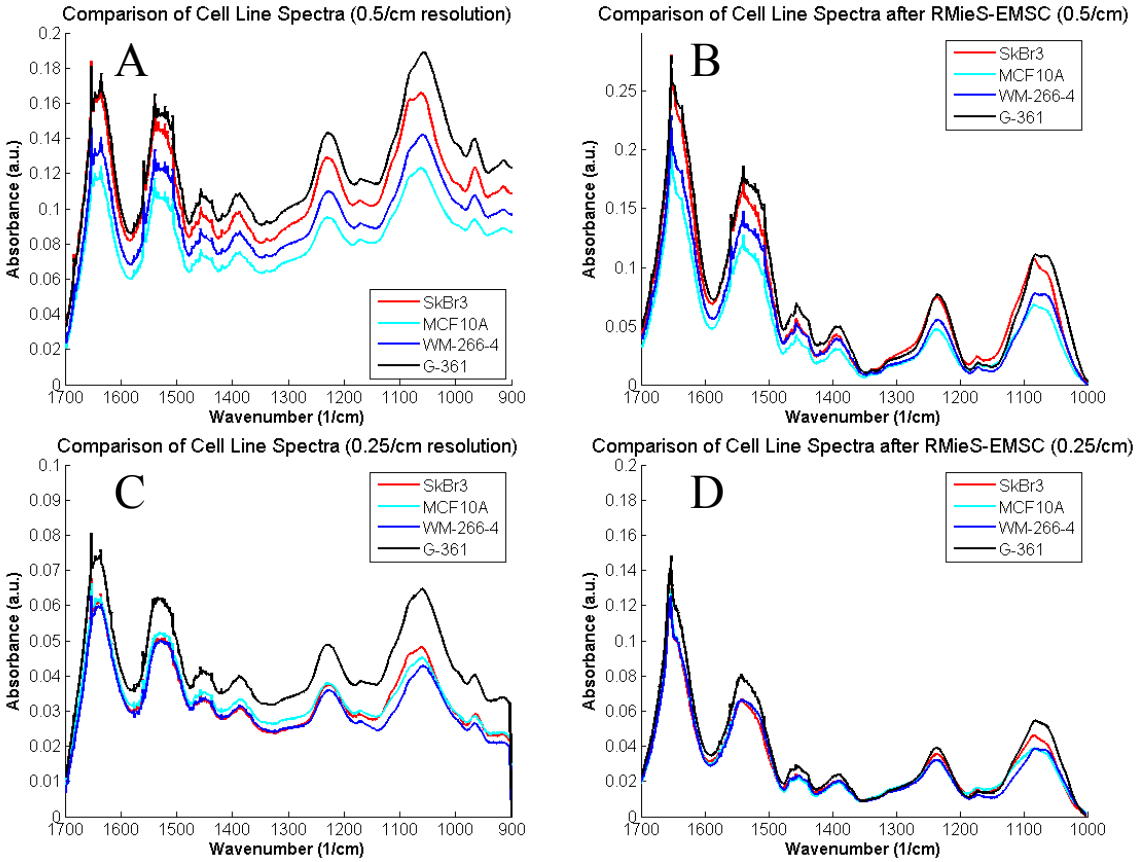

Figure 20. Comparison of cell lines with DI rinse at different resolutions before and after RMieS-EMSC. It is hard to tell how similar the two runs are before the sample correction is done (A and C), after the sample correction the two runs look much more similar (B and D). It is also much easier to actually visually see the differences in peak height between the cell lines.